

Hydrolysis of Tri-*tert*-butylaluminum: The First Structural Characterization of Alkylalumoxanes [(R₂Al)₂O]_n and (RAIO)_n

Mark R. Mason,^{1a} Janna M. Smith,^{1b} Simon G. Bott,^{1b} and Andrew R. Barron^{*,1a}

Contribution from the Department of Chemistry, Harvard University, Cambridge, Massachusetts 02138, and Department of Chemistry, University of North Texas, Denton, Texas 76203

Received December 17, 1992

Abstract: *tert*-Butyl-substituted alumoxanes have been prepared and characterized by multinuclear magnetic resonance spectroscopy, mass spectrometry, and X-ray crystallography. The low-temperature (-78 °C) hydrolysis of Al(^tBu)₃ in pentane results in the formation of the trimeric hydroxide [(^tBu)₂Al(μ-OH)]₃ (**1**) as the major product. Hydrated salt hydrolysis of Al(^tBu)₃ in toluene followed by thermolysis of the reaction mixture yields the tetrameric alumoxane [(^tBu)₂Al{μ-OAl(^tBu)₂}]₂ (**2**) and the octameric alumoxane [(^tBu)Al(μ₃-O)]₈ (**3**). In contrast the thermolysis of **1** yields the hexameric and nonameric alumoxanes, [(^tBu)Al(μ₃-O)]₆ (**4**) and [(^tBu)Al(μ₃-O)]₉ (**5**). Dissolution of compound **1** in THF or MeCN yields the hydrogen-bound complexes [(^tBu)₂Al(μ-OH)]₃·2THF (**6**) and [(^tBu)₂Al(μ-OH)]₃·2MeCN (**7**), respectively, while no adduct is observed in Et₂O solution. The reaction of **1** with pyridine results in a disproportionation reaction to yield the dimeric compound [(^tBu)₂Al(py)]₂(μ-O) (**8**). Compound **8** may be prepared directly from the partial hydrolysis of Al(^tBu)₃ in pyridine, in which it exists as the Lewis acid-base complex Al(^tBu)₃(py) (**9**), or from the addition of pyridine to **2**. The molecular structures of compounds **1**, **2**, **4**, and **6-8** have been determined by X-ray crystallography. The relationship between the *tert*-butylalumoxanes and the Kaminsky cocatalyst methylalumoxane, MAO, is discussed. Crystal data for **1**: monoclinic, C₂/c, *a* = 17.697(6), *b* = 10.198(6), *c* = 17.781(5) Å, β = 109.37(2)°, *Z* = 4, *R* = 0.0481, *R*_w = 0.0587. Crystal data for **2**: monoclinic, C₂/c, *a* = 41.622(3), *b* = 9.0176(8), *c* = 21.303(1) Å, β = 99.250(5)°, *Z* = 8, *R* = 0.0479, *R*_w = 0.0538. Crystal data for **4**: triclinic, P $\bar{1}$, *a* = 11.847(3), *b* = 12.208(2), *c* = 13.711(4) Å, α = 103.83(2), β = 109.02(1), γ = 92.37(3)°, *Z* = 2, *R* = 0.0689, *R*_w = 0.0972. Crystal data for **6**: monoclinic, P₂/c, *a* = 11.463(3), *b* = 15.603(6), *c* = 22.263(6) Å, β = 95.63(2)°, *Z* = 4, *R* = 0.0550, *R*_w = 0.0757. Crystal data for **7**: monoclinic, P₂/n, *a* = 11.406(2), *b* = 21.297(7), *c* = 14.972(2) Å, β = 96.76(2)°, *Z* = 4, *R* = 0.0381, *R*_w = 0.0408. Crystal data for **8**: triclinic, P $\bar{1}$, *a* = 9.074(2), *b* = 9.486(3), *c* = 9.728(3) Å, α = 104.28(2), β = 99.48(2), γ = 112.92(2)°, *Z* = 1, *R* = 0.0424, *R*_w = 0.0453.

Introduction

The controlled hydrolysis of aluminum alkyls yields industrially important oligomeric compounds of the formula (RAIO)_n. These oligomers belong to a general class of aluminum- and oxygen-containing materials called alumoxanes, species which contain at least one bridging oxo group between two aluminum centers.² Alkyl-substituted alumoxanes were extensively studied in the 1960s as active catalysts in the polymerization of epoxides,^{3,4} aldehydes,^{5,6} and olefins.^{7,8} Renewed interest in alkylalumoxanes was generated in the 1980s primarily from the work of Kaminsky and co-workers, who found methylalumoxane (MAO) to be a highly active cocatalyst for group 4 metallocene (e.g., Cp₂ZrMe₂) catalyzed ethylene and propylene polymerization.⁹ The role of the Lewis acidic MAO in these polymerizations is proposed to be alkyl abstraction, forming a "cation-like" metal center, i.e., [Cp₂ZrMe]⁺. This view is supported by XPS,¹⁰ NMR spectroscopic,¹¹ surface chemical,¹² and theoretical studies,¹³ as well as

the synthesis of highly active, well-characterized, cationic metal-alkyl polymerization catalysts.¹⁴⁻¹⁸

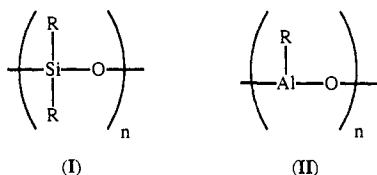
* Author to whom correspondence should be addressed.

- (1) (a) Harvard University. (b) University of North Texas.
 (2) Non-oxo-containing aluminum alkoxides are generally not included in this classification, although alumoxanes may contain a variety of pendant groups attached to aluminum. The term alumoxanes will in the present case, however, denote oligomeric species derived from the hydrolysis of aluminum alkyls, i.e., [(R₂Al)₂O]_n and (RAIO)_n; see: Barron, A. R. *Comments Inorg. Chem.* **1993**, *14*, 123.
 (3) (a) Colclough, R. O. *J. Polym. Sci.* **1959**, *34*, 178. (b) Colclough, R. O.; Gee, G.; Jagger, A. H. *J. Polym. Sci.* **1960**, *48*, 273.
 (4) Vandenberg, E. J. *J. Polym. Sci.* **1960**, *47*, 489.
 (5) Saegusa, T.; Fujii, Y.; Fujii, H.; Furukawa, J. *Makromol. Chem.* **1962**, *55*, 232.
 (6) Ishida, S. I. *J. Polym. Sci.* **1962**, *62*, 1.
 (7) Longiave, C.; Castelli, R. *J. Polym. Sci.* **1963**, *4C*, 387.
 (8) Sakharovskaya, G. B. *Zh. Obshch. Khim.* **1969**, *39*, 788.
 (9) See for example: (a) Sinn, H.; Kaminsky, W.; Vollmer, H. J.; Woldt, R. *Angew. Chem., Int. Ed. Engl.* **1980**, *92*, 390. (b) Sinn, H.; Kaminsky, W. *Adv. Organomet. Chem.* **1980**, *18*, 99.

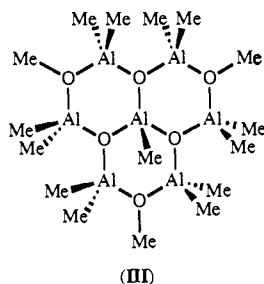
- (10) Gassman, P. G.; Callstrom, M. R. *J. Am. Chem. Soc.* **1987**, *109*, 7875.
 (11) (a) Sishta, C.; Hathorn, R. M.; Marks, T. J. *J. Am. Chem. Soc.* **1992**, *114*, 1112. (b) Resconi, L.; Bossi, S.; Abis, L. *Macromolecules* **1990**, *23*, 4489.
 (12) Dahmen, K. H.; Hedden, D.; Burwell, R. L., Jr.; Marks, T. J. *Langmuir* **1988**, *4*, 1212.
 (13) (a) Jolly, C. A.; Marynick, D. S. *J. Am. Chem. Soc.* **1989**, *111*, 7968.
 (b) Lauher, J. W.; Hoffmann, R. *J. Am. Chem. Soc.* **1976**, *98*, 1729.
 (14) (a) Horton, A. D.; Orpen, A. G. *Organometallics* **1992**, *11*, 8. (b) Horton, A. D.; Orpen, A. G. *Organometallics* **1991**, *10*, 3910. (c) Amorose, D. M.; Lee, R. A.; Petersen, J. L. *Organometallics* **1991**, *10*, 2191. (d) Taube, R.; Krukowka, L. *J. Organomet. Chem.* **1988**, *347*, C9. (e) Eisch, J. J.; Piotrowski, A. M.; Brownstein, S. K.; Gabe, E. J.; Lee, F. L. *J. Am. Chem. Soc.* **1985**, *107*, 7219.
 (15) (a) Bochmann, M.; Lancaster, S. J. *J. Organomet. Chem.* **1992**, *434*, C1. (b) Bochmann, M.; Jaggard, A. J. *J. Organomet. Chem.* **1992**, *424*, C5. (c) Bochmann, M.; Karger, G.; Jaggard, A. J. *J. Chem. Soc., Chem. Commun.* **1990**, 1038. (d) Bochmann, M.; Jaggard, A. J.; Nicholls, J. C. *Angew. Chem., Int. Ed. Engl.* **1990**, *29*, 780. (e) Bochmann, M.; Jaggard, A. J.; Hursthouse, M. B.; Mazid, M. *Polyhedron* **1990**, *9*, 2097. (f) Bochmann, M.; Jaggard, A. J.; Hursthouse, M. B.; Motevalli, M. *Polyhedron* **1989**, *8*, 1838. (g) Bochmann, M.; Wilson, L. M.; Hursthouse, M. B.; Motevalli, M. *Organometallics* **1988**, *7*, 1148. (h) Bochmann, M.; Wilson, L. M.; Hursthouse, M. B.; Short, R. L. *Organometallics* **1987**, *6*, 2556. (i) Bochmann, M.; Wilson, L. M. *J. Chem. Soc., Chem. Commun.* **1986**, 1610.
 (16) (a) Jordan, R. F. *Adv. Organomet. Chem.* **1991**, *32*, 325. (b) Alelyunas, Y. W.; Jordan, R. F.; Echols, S. F.; Borkowsky, S. L.; Bradley, P. K. *Organometallics* **1991**, *10*, 1406. (c) Jordan, R. F.; Taylor, D. F.; Baenziger, N. C. *Organometallics* **1990**, *9*, 1546. (d) Jordan, R. F.; LaPointe, R. E.; Bradley, P. K.; Baenziger, N. *Organometallics* **1989**, *8*, 2892. (e) Jordan, R. F. *J. Chem. Educ.* **1988**, *65*, 285. (f) Jordan, R. F.; Echols, S. F. *Inorg. Chem.* **1987**, *26*, 383. (g) Jordan, R. F.; LaPointe, R. E.; Bajgur, C. S.; Echols, S. F.; Willett, R. J. *Am. Chem. Soc.* **1987**, *109*, 4111. (h) Jordan, R. F.; Bajgur, C. S.; Dasher, W. E.; Rheingold, A. L. *Organometallics* **1987**, *6*, 1041. (i) Jordan, R. F.; Bajgur, C. S.; Willett, R.; Scott, B. J. *Am. Chem. Soc.* **1986**, *108*, 7410. (j) Jordan, R. F.; Dasher, W. E.; Echols, S. F. *J. Am. Chem. Soc.* **1986**, *108*, 1718.

Despite the increased understanding of the reactivity at the transition metal center in these catalyst systems, the structure of MAO remains ambiguous. Full characterization of MAO by NMR spectroscopy has been hindered by disproportionation reactions at high temperatures, association in solution to give a mixture of oligomers, and the presence of multiple equilibria.¹⁹ In addition, the inability to isolate crystalline samples has prevented characterization by X-ray diffraction. In fact, crystallographic data on alumoxanes is sparse and limited to the anionic alkyl compounds $[\text{Al}_7\text{O}_6\text{Me}_{16}]^-$,²⁰ $[\text{Me}_2\text{AlOAlMe}_3]_2^{2-}$,²¹ and $[\text{PhCO}_2(\text{Me}_2\text{Al})_2\text{OAlMe}_3]^-$,²² as well as a few examples stabilized by multidentate ligands, $[\text{L}_2\text{Al}]_2(\mu\text{-O})$, $\text{L} = 2\text{-methyl-8-quinolinolato}$,²³ $\text{L}_2 = \text{phthalocyaninato}$,²⁴ $N,N\text{-ethylenbis}(\text{salicylideneimine})$.²⁵

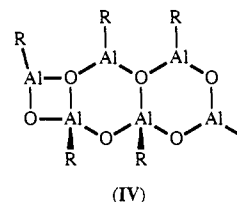
On the basis of the known structure of dialkylsiloxane polymers (I), alumoxanes were originally proposed to have a linear or cyclic chain structure consisting of alternating aluminum and oxygen atoms (II).¹⁹ Such a structure would obviously require the



aluminum to have a coordination number of three, which is rare, only existing in compounds in which oligomerization is sterically hindered by bulky ligands.²⁶ Since it is common for aluminum to maximize its coordination number through the formation of dimers and trimers via bridging ligands,²⁷ the majority of workers have proposed therefore that the aluminum must have a coordination number of at least four. The first crystallographic evidence for this was provided by Atwood et al. with their structural determination of the $[\text{Al}_7\text{O}_6\text{Me}_{16}]^-$ anion.²⁰ The anion consists of an Al_6O_6 ring capped by a seventh aluminum atom which is bonded to three alternate oxygen atoms in the ring (III). The

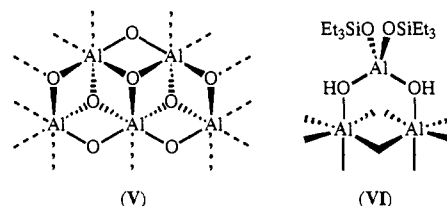


similarity of this structure to those of dimeric and trimeric dialkylaluminum alkoxide compounds, $[\text{R}_2\text{Al}(\mu\text{-OR})]_n$, has prompted many groups to propose structures based on either fused four- or six-membered rings or both, as illustrated for IV.¹⁹ While these models more closely follow the known chemistry of



aluminum,²⁸ and hence appear to be more reasonable than a linear chain structure, a significant problem remains. Despite the coordinative saturation of the core aluminum centers, the peripheral aluminum atoms remain three-coordinate. In order to overcome the deficiency in this structural model, the presence of alkyl bridges and/or additional trialkylaluminum groups has been suggested.^{19,29}

Two-dimensional structures had also been proposed for alkoxide-, siloxide-, and carboxylate-substituted alumoxanes.³⁰ We have shown, however, that hydrolytically stable alumoxanes of the formula $[\text{Al}(\text{O})_x(\text{OH})_y(\text{X})_z]_n$ ($\text{X} = \text{OSiR}_3, \text{O}_2\text{CR}$) are neither linear nor cyclic structures but three-dimensional clusters.³¹ On the basis of multinuclear NMR, IR, and X-ray photoelectron spectroscopic evidence, as well as a single-crystal X-ray diffraction study on $\text{Al}_{10}(\text{OH})_{16}(\text{OSiEt}_3)_{14}$, we have proposed that these non-alkylalumoxanes have a core isostructural to that of the minerals boehmite and diaspore, $[\text{Al}(\text{O})(\text{OH})]_n$, in which the core aluminums are six-coordinate (V), with, in the case of the siloxy derivatives, a periphery containing four-coordinate aluminum (e.g., VI).³¹



Aluminum-27 NMR spectroscopic measurements of MAO and related alkylalumoxanes show predominantly four-coordinate aluminum centers,¹⁹ thus precluding structures identical to those of the alkoxy-, siloxy-, or carboxylalumoxanes. However, some sort of a three-dimensional structure for alkylalumoxanes is an intriguing possibility, and one that has surprisingly *not been previously advanced*. Three-dimensional cluster or cage compounds are, in fact, quite common for many main group compounds.³² For the group 13 elements, these include the well-known iminoalanes, $[\text{RAl}(\mu_3\text{-NR}')_n]_n$,³³ and our recently reported gallium chalcogenide compounds, $[(\text{tBu})\text{Ga}(\mu_3\text{-E})]_n$ ($\text{E} = \text{S}, \text{Se}, \text{Te}$),³⁴⁻³⁶ each of which are isoelectronic to alkylalumoxanes of the formula $(\text{RAIO})_n$.

(28) Eisch, J. J. In *Comprehensive Organometallic Chemistry*; Wilkinson, G., Stone, F. G. A., Abel, E. W., Eds.; Pergamon Press: Oxford, England, 1982; Vol. 1, Chapter 6.

(29) Serwatowski, J. *Synthesis and Some Chemical Reactions of Tetraalkyldiboroxanes*; Wydawnictwa Politechniki Warszawskiej, 1989.

(30) See for example: (a) Kimura, Y.; Sugaya, S.; Ichimura, T.; Taniguchi, I. *Macromolecules* **1987**, *20*, 2329. (b) Kimura, Y.; Furukawa, M.; Yamane, H.; Kitao, T. *Macromolecules* **1989**, *22*, 79. (c) Kimura, Y.; Tanimoto, S.; Yamane, H.; Kitao, T. *Polyhedron* **1990**, *9*, 371.

(31) Applett, A. W.; Warren, A. C.; Barron, A. R. *Chem. Mater.* **1992**, *4*, 167.

(32) For a comprehensive review on cage compounds of main group metals, see: Veith, M. *Chem. Rev.* **1990**, *90*, 3.

(33) (a) Hitchcock, P. B.; Smith, J. D.; Thomas, K. M. *J. Chem. Soc., Dalton Trans.* **1976**, 1433. (b) Gosling, K.; Smith, J. D.; Wharmby, D. H. *J. Chem. Soc. A* **1969**, 1738. (c) Cucinella, S.; Salvatori, T.; Busetto, C.; Perego, G.; Mazzei, A. *J. Organomet. Chem.* **1974**, *78*, 185. (d) Cesari, M.; Perego, G.; Del Piero, G.; Cucinella, S.; Cernia, E. *J. Organomet. Chem.* **1974**, *78*, 203. (e) Del Piero, G.; Cesari, M.; Dozzi, G.; Mazzei, A. *J. Organomet. Chem.* **1977**, *129*, 281. (f) Del Piero, G.; Perego, G.; Cucinella, S.; Cesari, M.; Mazzei, A. *J. Organomet. Chem.* **1977**, *136*, 13. (g) Del Piero, G.; Cesari, M.; Perego, G.; Cucinella, S.; Cernia, E. *J. Organomet. Chem.* **1977**, *129*, 289. (h) Amirkhalili, S.; Hitchcock, P. B.; Smith, J. D. *J. Chem. Soc., Dalton Trans.* **1979**, 1206.

(17) (a) Yang, X.; Stern, C. L.; Marks, T. J. *J. Am. Chem. Soc.* **1991**, *113*, 3623. (b) Yang, X.; Stern, C. L.; Marks, T. J. *Organometallics* **1991**, *10*, 840.

(18) (a) Hlatky, G. G.; Eckman, R. R.; Turner, H. W. *Organometallics* **1992**, *11*, 1413. (b) Hlatky, G. G.; Turner, H. W.; Eckman, R. R. *J. Am. Chem. Soc.* **1989**, *111*, 2728. (c) Turner, H. W.; Hlatky, G. G. *Eur. Pat. Appl.* 0 277 004, 1988. (d) Turner, H. W.; Hlatky, G. G. *Eur. Pat. Appl.* 0 277 003, 1988.

(19) Pasykiewicz, S. *Polyhedron* **1990**, *9*, 429.

(20) Atwood, J. L.; Hrcncir, D. C.; Priester, R. D.; Rogers, R. D. *Organometallics* **1983**, *2*, 985.

(21) Atwood, J. L.; Zaworotko, M. J. *J. Chem. Soc., Chem. Commun.* **1983**, 302.

(22) Bott, S. G.; Coleman, A. W.; Atwood, J. L. *J. Am. Chem. Soc.* **1986**, *108*, 1709.

(23) Kushi, Y.; Fernando, Q. J. *J. Chem. Soc., Chem. Commun.* **1969**, 555.

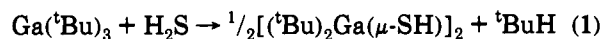
(24) Wynne, K. J. *Inorg. Chem.* **1985**, *24*, 1339.

(25) Gurian, P. L.; Cheatham, L. K.; Ziller, J. W.; Barron, A. R. *J. Chem. Soc., Dalton Trans.* **1991**, 1449.

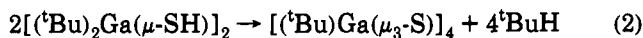
(26) Healy, M. D.; Barron, A. R. *Angew. Chem., Int. Ed. Engl.* **1992**, *31*, 921 and references therein.

(27) Oliver, J. P.; Kumar, R. *Polyhedron* **1990**, *9*, 409.

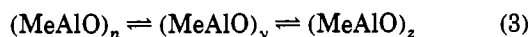
It is our recent results with gallium chalcogenide cage compounds that has offered us some insight into the possible structures of MAO and related alkylaluminumoxanes. The reaction of $\text{Ga}(\text{tBu})_3$ with H_2S (eq 1) yielded the first isolable gallium



hydrosulfido complex.³⁴ The hydrosulfido complex decomposes in both the solid state and solution to give the cubane $[(\text{tBu})\text{Ga}(\mu_3\text{-S})]_4$ (eq 2).^{34,35} Furthermore we have shown that the gallium



sulfido cubane undergoes a series of controlled topological structural rearrangements to yield $[(\text{tBu})\text{Ga}(\mu_3\text{-S})]_n$ ($n = 6, 7, 8$).³⁶ The structural rearrangements of $[(\text{tBu})\text{Ga}(\mu_3\text{-S})]_n$ have obvious relationships to aluminumoxanes, since it is a commonly accepted proposal that MAO, and related alkylaluminumoxanes, exist as equilibrium mixtures of oligomeric species (eq 3).¹⁹ Therefore,



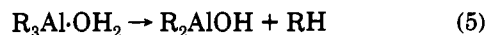
we may propose from these gallium sulfido homologues that alkylaluminumoxanes exist as three-dimensional clusters. Encouraged by our gallium chalcogenide³⁴⁻³⁶ and non-alkylaluminumoxane³¹ results, as well as the considerable literature precedence for main group cage compounds,³² we embarked on a program aimed at the investigation of the Al-O analogues to our Ga-S clusters.

Results and Discussion

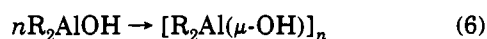
Hydrolysis of $\text{Al}(\text{tBu})_3$. The hydrolysis of AlR_3 ($\text{R} = \text{Me}, \text{Et}, \text{tBu}$) has been shown by variable-temperature ^1H NMR spectroscopy to proceed with the formation of an alkylaluminum-water complex (eq 4),³⁷ which subsequently eliminates alkane to



form a dialkylaluminum hydroxide complex (eq 5). The resulting

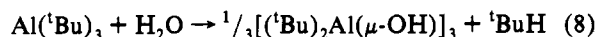


hydroxide complex rapidly associates to give dimers or larger oligomers in solution (eq 6). Further alkane elimination is



observed with the formation of alkylaluminumoxanes as these solutions are warmed to room temperature (eq 7).³⁷ Although the existence of alkylaluminum hydroxide intermediates is supported by solution NMR data, none have previously been isolated.

The reaction of $\text{Al}(\text{tBu})_3$ ³⁸ with 1 molar equiv of water results in the liberation of isobutane³⁹ and the formation of the trimeric aluminum hydroxide $[(\text{tBu})_2\text{Al}(\mu\text{-OH})]_3$ (**1**) (eq 8). It should be



noted, however, that while the hydrolysis of $\text{Ga}(\text{tBu})_3$ leads to

(34) Power, M. B.; Barron, A. R. *J. Chem. Soc., Chem. Commun.* **1991**, 1315.

(35) Power, M. B.; Ziller, J. W.; Tyler, A. N.; Barron, A. R. *Organometallics* **1992**, *11*, 1055.

(36) Power, M. B.; Ziller, J. W.; Barron, A. R. *Organometallics* **1992**, *11*, 2783.

(37) Boleslawski, M.; Serwatowski, J. *J. Organomet. Chem.* **1983**, *255*, 269.

(38) (a) Uhl, W. Z. *Anorg. Allg. Chem.* **1989**, *570*, 37. (b) Lehmkuhl, H.; Olbrysch, O.; Nehl, H. *Liebigs Ann. Chem.* **1973**, *708*. (c) Lehmkuhl, H.; Olbrysch, O. *Liebigs Ann. Chem.* **1973**, *715*.

(39) The ^1H NMR spectrum of a C_6D_6 solution of $\text{Al}(\text{tBu})_3$, immediately following addition of H_2O , reveals a doublet (δ 0.85) and multiplet (δ 1.62) consistent with isobutane.

Table I. Heteroatom NMR Chemical Shifts of *tert*-Butylaluminumoxanes and Related Compounds^a

compound	^{17}O	^{27}Al
$\text{Al}(\text{tBu})_3$		255 (6100) ^b
$\text{Al}(\text{tBu})_3(\text{py})$ (9)		154 (3200)
$[(\text{tBu})_2\text{Al}(\mu\text{-OH})]_3$ (1)	1 (195)	139 (5900)
$[(\text{tBu})_2\text{Ga}(\mu\text{-OH})]_3$	-17 (68)	
$[(\text{tBu})_2\text{Al}(\mu\text{-OH})]_3\cdot 2\text{THF}$ (6)	0 (650)	143 (5800)
$[(\text{tBu})_2\text{Al}(\mu\text{-OH})]_3\cdot 2\text{MeCN}$ (7)	2 (675)	140 (7200)
$[(\text{tBu})_2\text{Al}(\mu\text{-OAl}(\text{tBu})_2)]_2$ (2)	75 (3500)	142 (5200), 200 ^c
$[\text{Et}_2\text{Al}(\mu\text{-OAlEt}_2)]_2$ ^d	59 ^e	156 ^e
$[(\text{tBu})_2\text{Al}(\mu\text{-O}^i\text{tBu})]_2$		139 (2610)
$[(\text{tBu})_2\text{Al}(\text{py})]_2(\mu\text{-O})$ (8)	17 (200)	126 (5900)
$[(\text{H})\text{Al}(\mu_3\text{-N}^i\text{tBu})]_n$ ^f		122 ^e
$[(\text{tBu})\text{Al}(\mu_3\text{-O})]_6$ (4)	55 (500)	112 (7000)
$[(\text{H})\text{Al}(\mu_3\text{-N}^i\text{Pr})]_n$ ^g		123 ^e
$[(\text{H})\text{Al}(\mu_3\text{-NEt})]_n$ ^g		158 ^e
$[(\text{tBu})\text{Al}(\mu_3\text{-O})]_9$ (5)	74 (500, 3 O), 55 (500, 6 O)	120 (6500)
$[(\text{tBu})\text{Ga}(\mu_3\text{-O})]_9$	63 (700, 3 O), 48 (700, 6 O)	
$[(\text{Me})\text{AlO}]_n$ ^f	55 (800)	149 (1750)
$[(\text{Me})\text{AlO}]_n$ ^g		152 (1750)
$[(\text{tBu})\text{AlO}]_n$ ^h	70.4 (1200)	149 (7400)

^a $W_{1/2}$ values in Hz are given in parentheses. ^b Benn, R.; Rufinska, A.; Lehmkuhl, H.; Janssen, E.; Kruger, C. *Angew. Chem., Int. Ed. Engl.* **1983**, *22*, 779. ^c Spectra measured at 75 °C. ^d Serwatowski, J. ref 29. ^e No line widths reported. ^f Reference 64. ^g Hydrolysis of AlMe_3 (see Experimental Section). ^h Akzo Chemicals. ^h Hydrolysis of $\text{Al}(\text{tBu})_3$ (see Experimental Section).

$[(\text{tBu})_2\text{Ga}(\mu\text{-OH})]_3$ in quantitative yield,⁴⁰ the hydrolysis of $\text{Al}(\text{tBu})_3$ results in multiple products with **1** being isolated in yields which range from 20 to 55%. We have been unable to isolate these additional hydrolysis products; however, their identity has been confirmed in part from ^1H NMR spectroscopy, see below. Compound **1** is susceptible to slow decomposition in the solid state at room temperature under an inert atmosphere and is thus best stored cold (-20 °C) or used immediately following isolation.

The presence of a hydroxyl group in compound **1** is substantiated by a singlet ^1H NMR resonance at 2.02 ppm and a sharp O-H stretch (3584 cm^{-1}) in the infrared spectrum. The ^{17}O NMR spectrum of **1** shows a singlet (δ 1) somewhat downfield of that observed for the gallium analogue (δ -17). Unlike the case of the gallium compound,⁴⁰ we were unable to observe an ^{17}O - ^1H coupling, presumably due to the larger line width observed for **1** ($W_{1/2} = 195$ Hz) than for $[(\text{tBu})_2\text{Ga}(\mu\text{-OH})]_3$ ($W_{1/2} = 68$ Hz). The ^{27}Al NMR spectrum of **1** exhibits a broad resonance at 139 ppm consistent with association of the hydroxide monomers to give a four-coordinate aluminum center (see Table I). The trimeric nature of **1** in the gas phase is indicated by the presence of a molecular ion peak in the CI mass spectrum (see Experimental Section) and confirmed for the solid state by X-ray crystallography.

The molecular structure of compound **1** is shown in Figure 1. Selected bond lengths and angles are given in Table II. Half of the molecule is present in the asymmetric unit due to a crystallographically imposed C_2 symmetry, such that Al(1) and O(2) are on the axis. The Al_3O_3 ring is planar with the maximum deviation of the oxygen atoms from a plane defined by the three aluminum atoms being <0.005 Å. The hexagonal Al_3O_3 ring is distorted, with the average intra-ring angle at oxygen (142°) being significantly larger than that at aluminum (98°). While this difference is consistent with the relative hybridization at oxygen (sp^2) versus aluminum (sp^3), the angle at oxygen is significantly larger than either that found in the gas-phase electron diffraction determination of $[\text{Me}_2\text{Al}(\mu\text{-OMe})]_3$ (125.8°)⁴¹ or that

(40) Power, M. B.; Cleaver, W. M.; Apblett, A. W.; Barron, A. R.; Ziller, J. W. *Polyhedron* **1992**, *11*, 477.

(41) Drew, D. A.; Haaland, A.; Weidlein, J. Z. *Anorg. Allg. Chem.* **1973**, *398*, 241.

Table II. Selected Bond Lengths (Å) and Angles (deg) for [(^tBu)₂Al(μ-OH)]₃ (1)

Al(1)–O(1)	1.846(3)	Al(1)–C(11)	1.997(4)
Al(1)–O(1a)	1.846(3)	Al(1)–C(11a)	1.997(4)
Al(2)–O(1)	1.849(3)	Al(2)–O(2)	1.851(2)
Al(2)–C(21)	1.989(4)	Al(2)–C(25)	1.992(5)
O(1)–Al(1)–C(11)	110.8(2)	O(1)–Al(1)–O(1a)	98.1(2)
O(1)–Al(1)–C(11a)	108.6(2)	C(11)–Al(1)–O(1a)	108.6(2)
C(11)–Al(1)–C(11a)	118.1(2)	O(1a)–Al(1)–C(11a)	110.8(2)
O(1)–Al(2)–O(2)	97.9(2)	O(1)–Al(2)–C(21)	109.1(1)
O(1)–Al(2)–C(25)	110.2(2)	O(2)–Al(2)–C(21)	110.2(2)
O(2)–Al(2)–C(25)	109.0(2)	C(21)–Al(2)–C(25)	118.5(3)
Al(1)–O(1)–Al(2)	142.1(2)	Al(2)–O(2)–Al(2a)	141.9(2)

calculated for the model compound [H₂Al(μ-OH)]₃ (127.8°).⁴² An explanation for the unusually large Al–O–Al angle in **1** may be as follows: the presence of significant intramolecular *tert*-butyl repulsion not only favors a planar Al₃O₃ ring but causes an increase in the intra-ring Al...Al distance, 3.49 Å as compared to 3.305 Å and 3.29 Å calculated for [H₂Al(μ-OH)]₃ and observed for [Me₂Al(μ-OMe)]₃, respectively. Since the Al–O bond distances remain invariant (ca. 1.84–1.85 Å), as do the O...O distances (ca. 2.79 Å), the Al–O–Al angle must increase to accommodate the interligand steric interactions.

As noted above, while the hydrolysis of AlR₃ (R = Me, Et, ^tBu) has been shown to occur via hydroxide compounds,³⁷ the final product of the hydrolysis at room temperature is an alumoxane. Given the isolable nature of compound **1**, it may be assumed that higher temperatures are required for the formation of *tert*-butyl-substituted alumoxanes. Thus, we chose an alternate hydrolysis route which utilizes a higher reaction temperature and a hydrated metal salt. Hydrolysis of aluminum alkyls by hydrated metal salts such as Cu(SO₄)·5H₂O and Al₂(SO₄)₃·18H₂O is a mild, widely used route for alumoxane synthesis.⁴³ The low-temperature (–78 °C) addition of Al(^tBu)₃ to Al₂(SO₄)₃·18H₂O in toluene, followed by refluxing, yields a mixture of products from which compounds **2** and **3** may be separated by fractional crystallization as the major and minor products isolated, respectively.

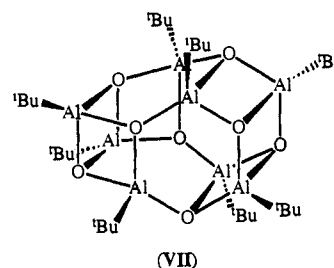
The ¹H and ¹³C NMR spectra of **2** indicate the presence of two equimolar aluminum-bound *tert*-butyl environments. Hydroxyl groups are absent from **2** on the basis of ¹H NMR and IR spectra. A four-coordinate aluminum center is indicated by a broad resonance at 142 ppm in the ²⁷Al NMR spectrum consistent with a four-coordinate aluminum center in a R₂AlO₂ coordination environment. While the presence of a Lewis-acidic, three-coordinate aluminum center is suggested by the reactivity of **2** with pyridine (see below), a resonance for a three-coordinate aluminum center was not observed in the ²⁷Al NMR spectrum at room temperature. However, warming the NMR sample to 80 °C results in sharpening of the resonance and the concurrent appearance of a second broad resonance at 200 ppm. This chemical shift is comparable to those reported for other three-coordinate aluminum compounds with a R₂AlO coordination environment (δ 180–200).⁴⁴ Thus, the ²⁷Al NMR spectrum of **2** is consistent with the presence of two aluminum coordination environments, one four-coordinate and the other three-coordinate. The ¹⁷O NMR spectrum of **2** shows a broad resonance at 75 ppm, within the range observed for a tricoordinate oxo ligand, Al₃(μ₃-O) (see Table I). The EI mass spectrum of **2** exhibits a fragment

Table III. Selected Bond Lengths (Å) and Angles (deg) for [(^tBu)₂Al{μ-OAl(^tBu)}₂]₂ (2)

Al(1)–O(1)	1.867(3)	Al(1)–O(2)	1.871(4)
Al(1)–C(11)	2.026(6)	Al(1)–C(15)	2.019(6)
Al(2)–O(1)	1.860(4)	Al(2)–O(2)	1.862(3)
Al(2)–C(21)	2.013(6)	Al(2)–C(25)	2.024(6)
Al(3)–O(1)	1.751(3)	Al(3)–C(31)	1.996(6)
Al(3)–C(35)	1.981(7)	Al(4)–O(2)	1.750(3)
Al(4)–C(41)	1.981(7)	Al(4)–C(45)	1.987(7)
O(1)–Al(1)–O(2)	84.2(1)	O(1)–Al(1)–C(11)	129.0(2)
O(1)–Al(1)–C(15)	100.0(2)	O(2)–Al(1)–C(11)	101.8(2)
O(2)–Al(1)–C(15)	128.0(2)	C(11)–Al(1)–C(15)	113.7(2)
O(1)–Al(2)–O(2)	84.7(1)	O(1)–Al(2)–C(21)	101.1(2)
O(1)–Al(2)–C(25)	128.7(2)	O(2)–Al(2)–C(21)	127.5(2)
O(2)–Al(2)–C(25)	100.9(2)	C(21)–Al(2)–C(25)	113.7(2)
O(1)–Al(3)–C(35)	119.9(2)	O(1)–Al(3)–C(35)	119.9(2)
C(31)–Al(3)–C(35)	120.2(3)	O(2)–Al(4)–C(41)	120.1(2)
O(2)–Al(4)–C(45)	120.0(2)	C(41)–Al(4)–C(45)	119.9(2)
Al(1)–O(1)–Al(2)	95.7(1)	Al(1)–O(1)–Al(3)	131.8(2)
Al(2)–O(1)–Al(3)	132.5(2)	Al(1)–O(2)–Al(2)	95.4(1)
Al(1)–O(2)–Al(4)	132.2(2)	Al(2)–O(2)–Al(4)	132.3(2)

(*m/z* = 539, 100%) consistent with loss of a *tert*-butyl substituent from a parent ion (not observed) with the composition ^tBu₈Al₄O₂. Loss of an alkyl substituent from the molecular ion is the most commonly observed fragmentation for alkylalumoxanes and is the major fragmentation observed in all of the alumoxanes reported herein. The analytical and spectroscopic characterization of **2** is consistent with the tetraaluminum structure [(^tBu)₂Al{μ-OAl(^tBu)}₂]₂, which has been confirmed by X-ray crystallography (see below).

The mass spectrum of compound **3** is consistent with an octameric alumoxane [(^tBu)Al(μ₃-O)]₈ (see Experimental Section), while the presence of two resonances for the *tert*-butyl groups in the ¹H and ¹³C NMR spectra (see Experimental Section) suggests a structure (VII) analogous to that reported for [HAl(μ₃-NⁿPr)]₈ and [MeAl(μ₃-NMe)]₈.^{33b,h} Unfortunately we were unable to obtain crystals of **3** suitable for X-ray diffraction.



The molecular structure of [(^tBu)₂Al{μ-OAl(^tBu)}₂]₂ (**2**) is shown in Figure 2; selected bond lengths and angles are given in Table III. The Al₄O₂ core is essentially planar with intra-ring Al–O distances of [1.860(4) – 1.871(4) Å], and significantly shorter exocyclic Al–O distances [Al(3)–O(1) = 1.751(3) Å, Al(4)–O(2) = 1.750(3) Å]. The intra-ring distances are toward the high end of the range associated with the Al₂O₂ cyclic structure (1.83–1.86 Å),²⁷ and the exocyclic distances are longer than those observed for other three-coordinate aluminum centers (1.64–1.68 Å),²⁶ both of these observations are consistent with significant steric interaction between *tert*-butyl groups on adjacent aluminum atoms.

While the Al₄O₂ core has been reported previously in a number of compounds, structural characterization has been obtained only

(42) Rogers, J. H.; Apblett, A. W.; Cleaver, W. M.; Tyler, A. N.; Barron, A. R. *J. Chem. Soc., Dalton Trans.* **1992**, 3179.

(43) (a) Collins, S.; Gauthier, W. J.; Holden, D. A.; Kuntz, B. A.; Taylor, N. J.; Ward, D. G. *Organometallics* **1991**, *10*, 2061. (b) Kaminsky, W.; Haehnsen, H. Ger. Offen. DE 3,240,383. (c) Razuvaev, G. A.; Sangalov, Yu. A.; Nel'kenbaum, Yu. Ya.; Minsker, K. S. *Izv. Akad. Nauk SSSR, Ser. Khim.* **1975**, 2547.

(44) Benn, R.; Janssen, E.; Lehmkuhl, H.; Rufinska, A.; Angermund, K.; Betz, P.; Goddard, R.; Krüger, C. *J. Organomet. Chem.* **1991**, *411*, 37.

(45) Thewalt, U.; Stollmaier, F. *Angew. Chem. Suppl.* **1982**, 209.

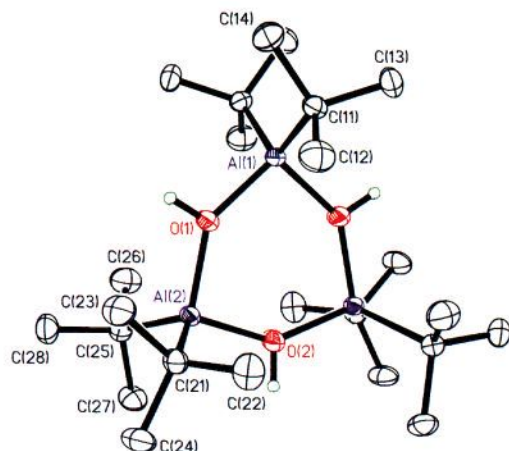


Figure 1. Molecular structure of $[(t\text{Bu})_2\text{Al}(\mu\text{-OH})_3]$ (**1**). Thermal ellipsoids are drawn at the 50% level, and the hydrogen atoms of the *tert*-butyl groups are omitted for clarity.

for the anions $[\text{Me}_2\text{Al}(\mu\text{-OAlMe}_3)]_2^{2-}$ ²¹ and $[\text{Cl}_2\text{Al}(\mu\text{-OAlCl}_3)]_2^{2-}$ ⁴⁵ and for the aluminum hydride $[\{(\eta^5\text{-C}_5\text{Me}_5)(\eta^5\text{-C}_5\text{Me}_4\text{CH}_2)\text{Ti}(\mu_2\text{-H})_2\text{Al}\}_2(\mu_3\text{-O})]_2$.⁴⁶ Compound **2**, however, represents not only the first structurally characterized example with two four-coordinate and two three-coordinate aluminum centers but also the first for a tetraalkyldialumoxane. It is reasonable to believe therefore that the structure proposed by Boleslawski and Serwatowski⁴⁷ for the isobutyl analogue (**VIII**) is possibly correct.

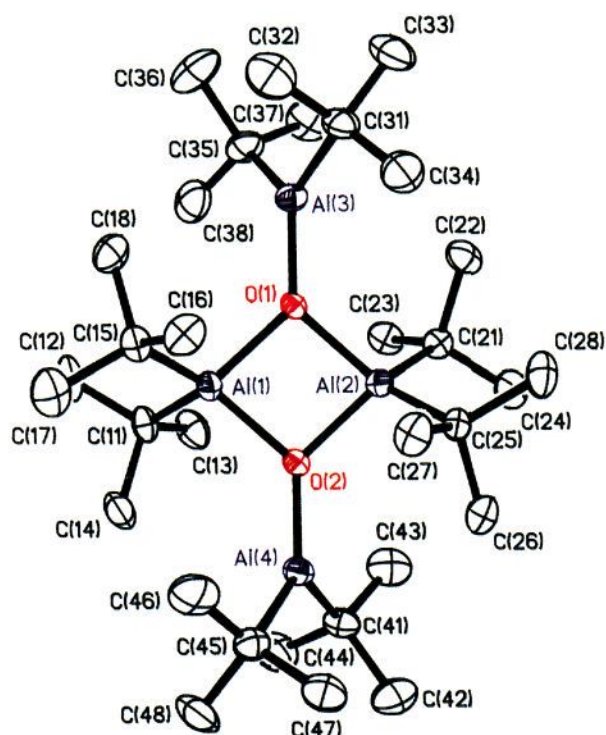
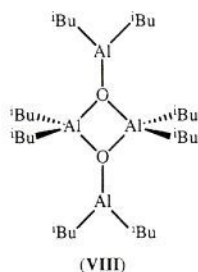


Figure 2. Molecular structure of $[(t\text{Bu})_2\text{Al}\{\mu\text{-OAl}(t\text{Bu})_2\}]_2$ (**2**). Thermal ellipsoids are drawn at the 30% level, and all the hydrogen atoms are omitted for clarity.

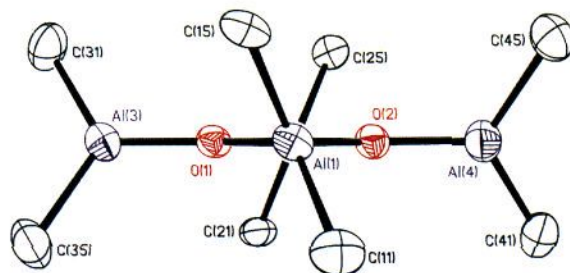
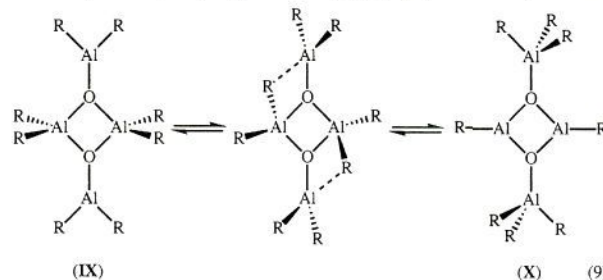


Figure 3. Partial coordination sphere of $[(t\text{Bu})_2\text{Al}\{\mu\text{-OAl}(t\text{Bu})_2\}]_2$ (**2**) viewed along the $\text{Al}(1)\cdots\text{Al}(2)$ vector; the *tert*-butyl methyl groups are omitted for clarity.

There has now been a wide range of dimeric di-*tert*-butyl group 13 compounds structurally characterized, $[(t\text{Bu})_2\text{M}(\mu\text{-X})]_2$ ($\text{X} = \text{OR}, \text{OOR}, \text{NR}_2, \text{PR}_2, \text{AsR}_2$).^{34,40,48} In each case the torsion angle between the MC_2 and M_2X_2 planes has been close to, or crystallographically equal to, 90° . In the case of compound **2**, the AlC_2 planes are pitched 67° [at $\text{Al}(1)$] and 68° [at $\text{Al}(2)$] with respect to the Al_2O_2 plane. As a result the four-coordinate aluminums are in a highly distorted tetrahedral geometry, as is clearly illustrated in Figure 3. Through observation of a CPK space-filling model, this distortion may be ascribed to the steric interactions between adjacent *tert*-butyl groups. The closest intramolecular $\text{C}\cdots\text{C}$ distances are between 3.74 and 3.84 Å, close to the sum of two methyl group van der Waals radii (4.0 Å).⁴⁹ We have previously observed a similar distortion at indium in the molecular structure of $[(2,4,6\text{-Me}_3\text{C}_6\text{H}_2)_2\text{In}(\mu\text{-Cl})]_2$.⁵⁰

The twisting of the substituents on the aluminum centers in compound **2** away from tetrahedral is also of interest with respect to the ligand redistribution reaction proposed to occur during the thermolysis of $[\text{Me}_2\text{Al}(\mu\text{-OAlMe}_2)]_2$ (eq 9, $\text{R} = \text{Me}$).¹⁹ This



alkyl exchange is undoubtedly facile for the methyl derivative, since the ability of methyl groups to act as bridging ligands via a three-center two-electron bond is well documented.⁵¹ The

(46) Lobkovskii, E. B.; Sizov, A. I.; Bulychev, B. M.; Sokolova, I. V.; Soloveichik, G. L. *J. Organomet. Chem.* **1987**, *319*, 69.

(47) Boleslawski, M.; Serwatowski, J. *J. Organomet. Chem.* **1983**, *254*, 159.

(48) Cleaver, W. M.; Barron, A. R. *J. Am. Chem. Soc.* **1989**, *111*, 8966.

(49) Pauling, L. *The Nature of the Chemical Bond*; Cornell University Press: Ithaca, NY, 1960; Chapter 7.

(50) Leman, J. T.; Barron, A. R. *Organometallics* **1989**, *8*, 2214.

(51) Oliver, J. P. In *Advanced Organometallic Chemistry*; Stone, F. G. A., West, R., Eds.; Academic Press: New York, 1977; p 235.

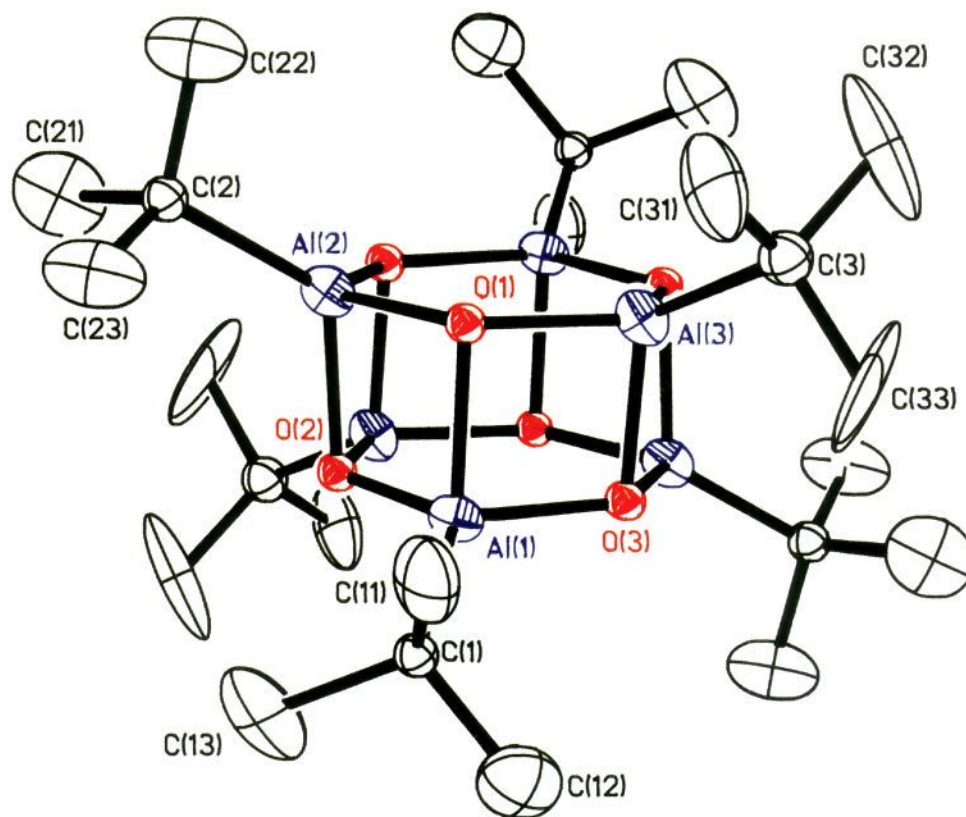
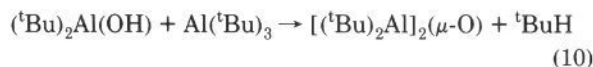


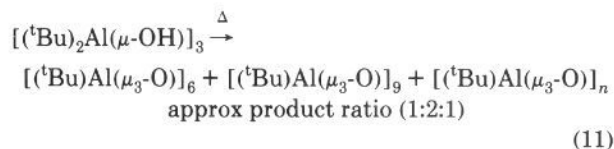
Figure 4. Molecular structure of one of the independent molecules of $[(t\text{Bu})\text{Al}(\mu_3\text{-O})]_6$ (**4**). Thermal ellipsoids are drawn at the 30% level, and all the hydrogen atoms are omitted for clarity.

substitution of *tert*-butyl for methyl groups inhibits the forward reaction shown in eq 9, thus allowing for the isolation of **2**. However, the contorted structure of **2** and the close α -carbon--aluminum contacts (3.73–3.80 Å) are suggestive of a model for the transition state in the interconversion of IX and X (eq 9).

Thermolysis of $[(t\text{Bu})_2\text{Al}(\mu\text{-OH})]_3$. The formation of compound **2** during the hydrolysis of $\text{Al}(t\text{Bu})_3$ suggests that under these reaction conditions the condensation of the hydroxide with $\text{Al}(t\text{Bu})_3$ (eq 10) occurs at a comparable rate to the condensation of the hydroxide intermediate (cf., eq 7). In an effort to circumvent this side reaction, the thermolysis of the isolated trimeric hydroxide was investigated.

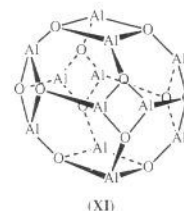


Thermolysis of a benzene-*d*₆ solution of $[(t\text{Bu})_2\text{Al}(\mu\text{-OH})]_3$ (**1**) results in the loss of isobutane and the formation of three main species which account for ca 90% of the *tert*-butyl groups by ¹H NMR spectroscopy (eq 11). It should be noted that the



thermolysis of **1** does not yield appreciable quantities of either **2** or **3**. On a preparative scale (see Experimental Section), these compounds may be readily separated by fractional crystallization. The identities of two of these products have been determined by NMR spectroscopy, mass spectrometry, and X-ray crystallography to be the hexameric and the nonameric alumoxanes,

$[(t\text{Bu})\text{Al}(\mu_3\text{-O})]_6$ (**4**) and $[(t\text{Bu})\text{Al}(\mu_3\text{-O})]_9$ (**5**), respectively. On the basis of mass spectrometry, the third component is of a higher molecular weight than compound **5**, i.e., $[(t\text{Bu})\text{Al}(\mu_3\text{-O})]_n$, where $n > 9$. Fragments consistent with $10M^+ - t\text{Bu}$ and $12M^+$ are observed in the EI mass spectrum, while the ¹H NMR spectrum indicates a single *tert*-butyl environment, suggesting a highly symmetrical compound. If we assume that this high-nuclearity species is a cage compound of the general formula $[(t\text{Bu})\text{Al}(\mu_3\text{-O})]_n$ (as indicated by mass spectrometry), then the value for $n > 9$ where all aluminum centers would be equivalent is 12, i.e., a dodecamer (XI). Iminoalane clusters, $[\text{RAl}(\mu_3\text{-NR}')_n]$, have been reported for $n = 4, 6\text{--}10, 15$, and 16 although no structural characterization above $n = 8$ is available.³³ We are at present attempting to isolate sufficient quantities to confirm this proposal by X-ray crystallography.



The molecular structure of $[(t\text{Bu})\text{Al}(\mu_3\text{-O})]_6$ (**4**) is shown in Figure 4; selected bond lengths and angles are given in Table IV. Two crystallographically independent molecules of **4** are present in the unit cell, each residing on a center of symmetry; Al(1)–Al(3) on (0,0,0) and Al(4)–Al(6) on $(\frac{1}{2}, \frac{1}{2}, \frac{1}{2})$. The Al_6O_6 core can be described as a hexagonal prism with alternating Al and O atoms. Unlike the chair conformation of the Ga_3S_3 faces in $[(t\text{Bu})\text{Ga}(\mu_3\text{-S})]_6$,³⁶ the Al_3O_3 hexagonal faces are essentially planar with significant trigonal distortion $[\text{O}–\text{Al}–\text{O}_{\text{av}} = 113^\circ$,

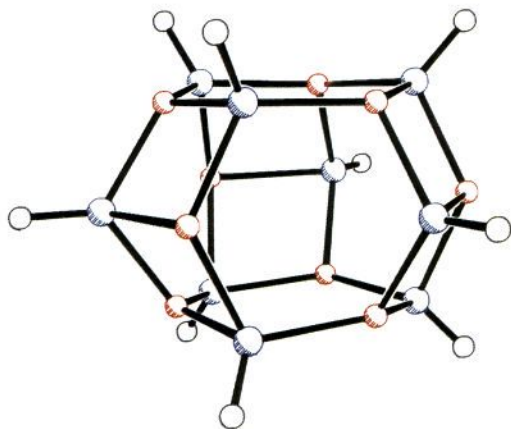


Figure 5. Molecular structure of $[(t\text{Bu})\text{Al}(\mu_3\text{-O})]_9$ (**5**); see Experimental Section. Methyl groups are omitted for clarity.

Table IV. Selected Bond Lengths (Å) and Angles (deg) for the Two Independent Molecules of $[(t\text{Bu})\text{Al}(\mu_3\text{-O})]_6$ (**4**)

Molecule 1			
Al(1)–O(1)	1.905(4)	Al(1)–O(2)	1.795(5)
Al(1)–O(3)	1.782(6)	Al(1)–C(1)	1.913(7)
Al(2)–O(1)	1.791(5)	Al(2)–O(2)	1.880(5)
Al(2)–O(3a)	1.778(5)	Al(2)–C(2)	1.92(1)
Al(3)–O(1)	1.760(6)	Al(3)–O(2a)	1.789(6)
Al(3)–O(3)	1.889(4)	Al(3)–C(3)	1.960(9)
Molecule 2			
Al(4)–O(4)	1.887(4)	Al(4)–O(5a)	1.802(6)
Al(4)–O(6)	1.795(6)	Al(4)–C(4)	1.937(9)
Al(5)–O(4a)	1.795(4)	Al(5)–O(5)	1.901(4)
Al(5)–O(6)	1.803(6)	Al(5)–C(5)	1.961(4)
Al(6)–O(4)	1.781(6)	Al(6)–O(5)	1.796(6)
Al(6)–O(6)	1.877(4)	Al(6)–C(6)	1.95(1)
Molecule 1			
O(1)–Al(1)–O(2)	86.3(2)	O(1)–Al(1)–O(3)	86.3(2)
O(2)–Al(1)–O(3)	112.2(3)	O(1)–Al(1)–C(1)	119.9(3)
O(2)–Al(1)–C(1)	123.1(3)	O(3)–Al(1)–C(1)	118.6(3)
O(1)–Al(2)–O(2)	87.2(2)	O(1)–Al(2)–O(3a)	86.3(2)
O(2)–Al(2)–O(3a)	112.2(2)	O(1)–Al(2)–C(2)	118.1(3)
O(2)–Al(2)–C(2)	124.4(3)	O(3)–Al(2)–C(2)	120.3(3)
O(1)–Al(3)–O(2a)	112.3(2)	O(1)–Al(3)–O(3)	87.4(2)
O(2a)–Al(3)–O(3)	85.2(2)	O(1)–Al(3)–C(3)	119.0(4)
O(2a)–Al(3)–C(3)	122.2(4)	O(3)–Al(3)–C(3)	120.8(3)
Al(1)–O(1)–Al(2)	92.4(2)	Al(1)–O(1)–Al(3)	92.7(3)
Al(2)–O(1)–Al(3)	127.7(3)	Al(1)–O(2)–Al(2)	93.1(2)
Al(1)–O(2)–Al(3a)	127.5(2)	Al(2)–O(2)–Al(3a)	94.1(2)
Al(1)–O(3)–Al(2a)	127.1(3)	Al(1)–O(3)–Al(3)	92.6(3)
Molecule 2			
O(4)–Al(4)–O(5a)	87.9(2)	O(4)–Al(4)–O(6)	86.6(2)
O(5)–Al(4)–O(6)	112.2(2)	O(4)–Al(4)–C(4)	120.9(3)
O(5)–Al(4)–C(4)	119.7(3)	O(6)–Al(4)–C(4)	120.5(3)
O(4)–Al(5)–O(5)	87.6(2)	O(4a)–Al(5)–O(6)	113.2(2)
O(5)–Al(5)–O(6)	87.6(2)	O(4a)–Al(5)–C(5)	119.6(3)
O(5)–Al(5)–C(5)	121.1(3)	O(6)–Al(5)–C(5)	119.2(3)
O(4)–Al(6)–O(5)	111.7(3)	O(4)–Al(6)–O(6)	87.3(2)
O(4)–Al(6)–C(6)	118.5(4)	O(5)–Al(6)–O(6)	88.6(2)
O(5)–Al(6)–C(6)	120.7(4)	O(6)–Al(6)–C(6)	122.2(3)
Al(2a)–O(3)–Al(3)	94.1(3)	Al(4)–O(4)–Al(5a)	92.0(2)
Al(4)–O(4)–Al(6)	92.7(2)	Al(5a)–O(4)–Al(6)	127.9(2)
Al(4a)–O(5)–Al(5)	91.4(2)	Al(4a)–O(5)–Al(6)	128.5(2)
Al(5)–O(5)–Al(6)	91.2(2)	Al(4)–O(6)–Al(5)	126.5(3)
Al(4)–O(6)–Al(6)	92.5(2)	Al(5)–O(6)–Al(6)	91.7(2)

Al–O–Al_{av} = 126°. A similar structure has been reported for the iminoalanes, $[\text{XAl}(\mu_3\text{-N}^i\text{Pr})]_6$ (X = H, Me, Cl).³³ The Al–O distances are of two types, those within [1.877(4)–1.905(5) Å] and those linking [1.760(6)–1.796(6) Å] the two Al_3O_3 rings. Both of these are longer than observed for two-coordinate oxide ligands^{23–25} but are comparable to those of the planar μ_3 -oxo groups in **2**. The ¹H, ¹³C, ¹⁷O, and ²⁷Al NMR spectra of **4** (see Table I and Experimental Section) are totally consistent with retention of the hexagonal prismatic structure in solution.

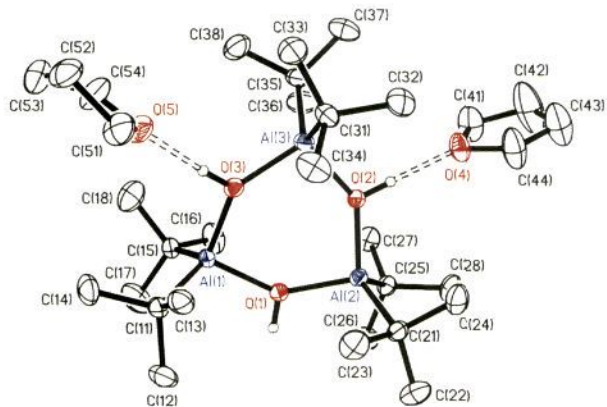


Figure 6. Molecular structure of $[(t\text{Bu})_2\text{Al}(\mu\text{-OH})]_3 \cdot 2\text{THF}$ (**6**). Thermal ellipsoids are drawn at the 40% level, and the non-hydroxide hydrogen atoms are omitted for clarity.

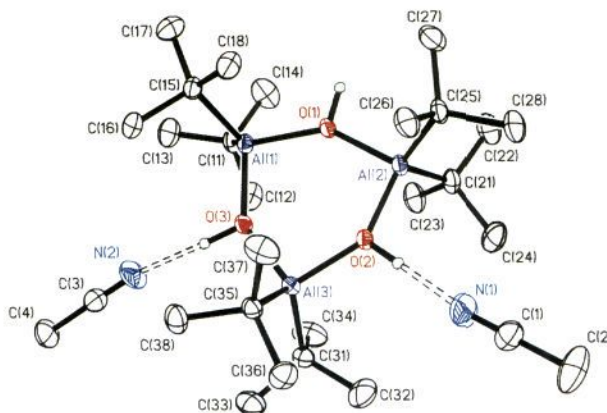


Figure 7. Molecular structure of $[(t\text{Bu})_2\text{Al}(\mu\text{-OH})]_3 \cdot 2\text{MeCN}$ (**7**). Thermal ellipsoids are drawn at the 40% level, and the non-hydroxide hydrogen atoms are omitted for clarity.

While X-ray crystallographic data was obtained for **5**, problems with refinement preclude a detailed analysis of the structure. However, as is discussed in the Experimental Section, the solution was sufficient to confirm the atomic connectivity, and this is shown in Figure 5. The cage structure consists of two parallel six-membered Al_3O_3 rings that are connected by three oxygen atoms and three aluminum atoms, such that every aluminum is four-coordinate and each oxygen has a coordination number of three. To the best of our knowledge, the only other nonameric, M_9X_9 , cage compounds of the main group metals to be reported are $[\text{Na}(\text{O}^i\text{Bu})]_9$ ⁵² and $[(t\text{Bu})\text{GaO}]_9$,³⁶ both of which are isostructural to **5**. The ¹H and ¹³C NMR spectra of **5** show the presence of two *tert*-butyl environments in a 1:2 ratio, while the ¹⁷O NMR spectrum (Table I) shows two oxide environments, again in a 1:2 ratio. Thus, the solution spectra confirm that the nonameric structure is retained in solution.

Reaction of $[(t\text{Bu})_2\text{Al}(\mu\text{-OH})]_3$ with Lewis Bases. Dissolution of $[(t\text{Bu})_2\text{Ga}(\mu\text{-OH})]_3$ in THF results in the formation of the monomeric hydroxide compound, $(t\text{Bu})_2\text{Ga}(\text{OH})(\text{THF})$.⁴⁰ In contrast, recrystallization of compound **1** from either neat THF or a pentane/THF mixture does not result in the formation of the Lewis acid–base complex, but of the solvate $[(t\text{Bu})_2\text{Al}(\mu\text{-OH})]_3 \cdot 2\text{THF}$ (**6**). Similarly, recrystallization of **1** from MeCN yields the solvated complex $[(t\text{Bu})_2\text{Al}(\mu\text{-OH})]_3 \cdot 2\text{MeCN}$ (**7**). The structures of compounds **6** and **7** have been confirmed by X-ray crystallography.

The molecular structures of **6** and **7** are shown in Figures 6 and 7; selected bond lengths and angles are given in Table V. Unlike the planar Al_3O_3 ring in **1**, those in compounds **6** and **7** exhibit a twist-boat conformation,⁵³ which can be readily seen



Figure 8. Core structure of $[(t\text{Bu})_2\text{Al}(\mu\text{-OH})]_3 \cdot 2\text{THF}$ (**6**) viewed along an $\text{Al}(3)\text{---O}(1)$ vector, showing both the twist-boat conformation of the Al_3O_3 ring and the positioning of the THF ligands. The *tert*-butyl methyl groups are omitted for clarity.

Table V. Selected Bond Lengths (Å) and Angles (deg) for $[(t\text{Bu})_2\text{Al}(\mu\text{-OH})]_3 \cdot 2\text{L}$

	L	
	THF (6)	MeCN (7)
Al(1)–O(1)	1.851(3)	1.857(2)
Al(1)–O(3)	1.836(3)	1.835(2)
Al(1)–C(11)	1.999(4)	2.002(3)
Al(1)–C(15)	1.996(4)	2.005(3)
Al(2)–O(1)	1.849(3)	1.860(2)
Al(2)–O(2)	1.831(3)	1.838(2)
Al(2)–C(21)	1.998(4)	1.998(3)
Al(2)–C(25)	1.989(4)	2.001(3)
Al(3)–O(2)	1.844(2)	1.839(2)
Al(3)–O(3)	1.844(3)	1.848(2)
Al(3)–C(31)	1.993(4)	2.001(3)
Al(3)–C(35)	2.000(4)	2.006(3)
O(1)–Al(1)–O(3)	97.8(1)	97.9(1)
O(1)–Al(1)–C(11)	111.0(1)	108.8(1)
O(1)–Al(1)–C(15)	106.2(1)	108.8(1)
O(3)–Al(1)–C(11)	109.3(1)	110.3(1)
O(3)–Al(1)–C(15)	114.1(1)	110.3(1)
C(11)–Al(1)–C(15)	116.8(2)	118.7(1)
O(1)–Al(2)–O(2)	98.5(1)	97.9(1)
O(1)–Al(2)–C(21)	107.9(1)	109.0(1)
O(1)–Al(2)–C(25)	110.7(1)	109.3(1)
O(2)–Al(2)–C(21)	112.2(1)	111.2(1)
O(2)–Al(2)–C(25)	110.7(1)	110.7(1)
C(21)–Al(2)–C(25)	116.8(2)	117.1(1)
O(2)–Al(3)–O(3)	99.3(1)	97.8(1)
O(2)–Al(3)–C(31)	109.9(1)	109.8(1)
O(2)–Al(3)–C(35)	109.8(1)	111.0(1)
O(3)–Al(3)–C(31)	110.1(1)	111.1(1)
O(3)–Al(3)–C(35)	110.1(1)	109.5(1)
C(31)–Al(3)–C(35)	116.2(2)	116.2(1)
Al(1)–O(1)–Al(2)	141.3(1)	141.0(1)
Al(2)–O(2)–Al(3)	139.8(1)	142.2(1)
Al(1)–O(3)–Al(3)	140.4(1)	142.0(1)

from Figure 8. As a consequence, the two hydrogen-bonded solvent molecules, THF (**6**) and MeCN (**7**), are positioned one above and one below the Al_3 plane. While the cone angle⁵⁴ of THF is significantly bigger than that of MeCN, it can be seen from Table V that the geometries of **6** and **7** are nearly identical, having chemically equivalent bond lengths, and angles being nearly structurally so. Since the distortion from a planar to a twist-boat conformation for the Al_3O_3 ring is undoubtedly due to the steric bulk of the Lewis base, a larger distortion from planarity might be expected for **6** as compared to **7**. This is not observed. However, consideration of the orientation of the THF ligands, i.e., perpendicular to the Al_3 plane, suggests that the ligand profile (the steric bulk taking into account ligand orientation) of THF

(53) Twist-boat conformations have been previously observed for six-membered 13/15 compounds $[\text{R}_2\text{MER}'_2]_3$; see for example: (a) Atwood, J. L.; Stucky, G. D. *J. Am. Chem. Soc.* **1970**, *92*, 285. (b) McLaughlin, G. M.; Sim, G. A.; Smith, J. D. *J. Chem. Soc., Dalton Trans.* **1972**, 2197. (c) Wells, R. L.; Purdy, A. P.; McPhail, A. T.; Pitt, C. G. *J. Organomet. Chem.* **1988**, *354*, 287. (d) Interrante, L. V.; Sigel, G. A.; Garbaskas, M.; Hejna, C.; Slack, G. A. *Inorg. Chem.* **1989**, *28*, 252.

(54) Tolman, C. A. *Chem. Rev.* **1977**, *77*, 313.

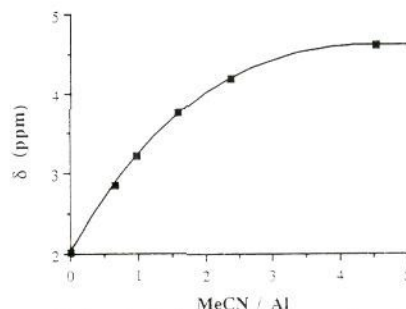
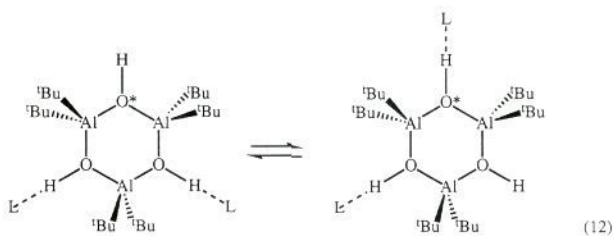


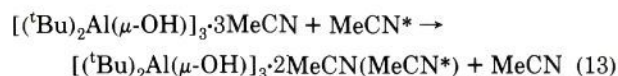
Figure 9. Hydroxide ^1H NMR chemical shift (δ) as a function of MeCN/Al ratio.

is in the present case close to that of MeCN, and thus the structural similarity of **6** and **7** is reasonable.

The IR spectra of **6** and **7** each show two $\nu(\text{OH})$ bands, one due to a free hydroxide [3690 cm^{-1} (**6**), 3594 cm^{-1} (**7**)] and one broad with increased intensity for the hydrogen-bonded hydroxide [3160 cm^{-1} (**6**), 3260 cm^{-1} (**7**)], consistent with the X-ray structural characterization. The ^1H NMR spectra of **6** and **7** show only a single resonance for the hydroxide groups [δ 3.42 (**6**), 3.56 (**7**)]. The solution NMR spectra are therefore consistent with the rapid and facile exchange of the Lewis base molecules [THF (**6**), MeCN (**7**)] with each of the three hydroxide groups (eq 12). This exchange process does not cease at $-60\text{ }^\circ\text{C}$.



The bis-solvates, **6** and **7**, are the only species isolated even from excess Lewis base. The reason for this is not immediately apparent, since consideration of space-filling models of **6** or **7** suggests that sufficient space is available for solvation by a third molecule of solvent. In order to investigate the formation of possible tris-complexes between **1** and Lewis bases, adduct formation has been monitored with the use of ^1H NMR spectroscopy. The chemical shift of the hydroxide moiety has been obtained as a function of the MeCN/Al molar ratio (Figure 9). The results show that, upon increasing the MeCN/Al molar ratio, there is a smooth downfield shift of the hydroxide resonance. The change in chemical shift levels off at a molar ratio consistent with $[(t\text{Bu})_2\text{Al}(\mu\text{-OH})]_3 \cdot 3\text{MeCN}$. The presence of a single resonance for the MeCN ligand in a solution of **1** with >3 equiv of MeCN suggests that free and coordinated MeCN are in rapid exchange (eq 13). This facile equilibrium is like that previously



observed for $[\text{Al}(\text{OSiPh}_3)_3(\text{H}_2\text{O})] \cdot 2\text{THF}$.⁵⁵ Given the coordination of 3 equiv of MeCN per aluminum trimer in solution, the isolation of **7** may be rationalized by assuming that the solubility of the bis-solvate is sufficiently less than those of the mono- or tris-solvate, promoting its preferential crystallization.

The formation of hydrogen-bonded aquo and hydroxide complexes during the hydrolysis of AlR_3 ($\text{R} = \text{Me}, \text{Et}, t\text{Bu}$) in diethyl ether solution has been previously noted.³⁷ However, we observe no evidence for complexation of Et_2O with **1**, consistent with a decrease in hydrogen bonding with increasing steric bulk of the aluminum alkyl group, i.e., $\text{Me} > \text{Et} > t\text{Bu}$.

(55) Apblett, A. W.; Warren, A. C.; Barron, A. R. *Can. J. Chem.* **1992**, *70*, 771.

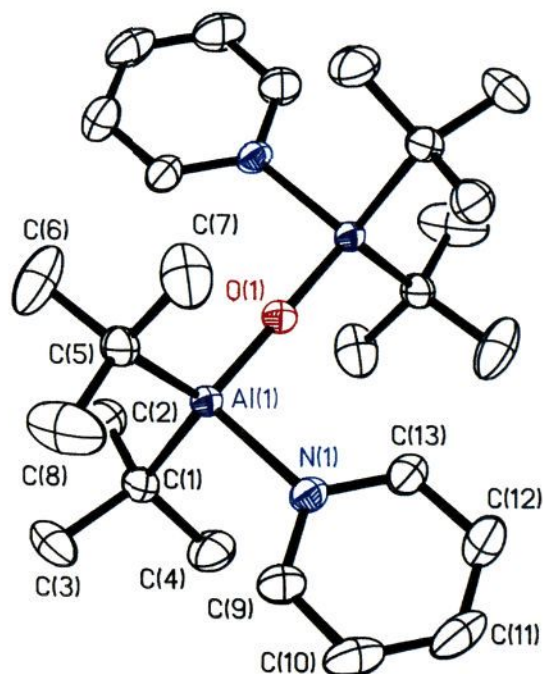
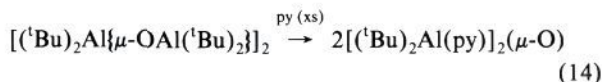


Figure 10. Molecular structure of $[(^t\text{Bu})_2\text{Al}(\text{py})]_2(\mu\text{-O})$ (**8**). Thermal ellipsoids are drawn at the 50% level, and all hydrogen atoms are omitted for clarity.

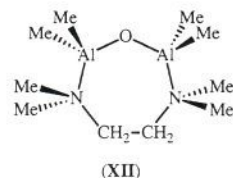
Although we have previously reported⁵⁶ that in the solid state the hydroxide moieties in the indium hydroxide cubane, $[(\text{Ph}_2\text{PO}_2)\text{InMe}(\mu_3\text{-OH})_4\cdot 4\text{py}]$, are hydrogen-bonded to solvating pyridine molecules, the reaction of **1** with pyridine does not result in the formation of the solvated complex. Instead the bright-yellow oxo-bridged dialuminum complex $[(^t\text{Bu})_2\text{Al}(\text{py})]_2(\mu\text{-O})$ (**8**) is formed in ca. 60% yield. The NMR and mass spectrometric data are entirely consistent with this structural formulation (see Table I and Experimental Section). Compound **8** may also be prepared by the partial hydrolysis of $\text{Al}(^t\text{Bu})_3(\text{py})$ (**9**) or by the addition of pyridine to compound **2** (eq 14).



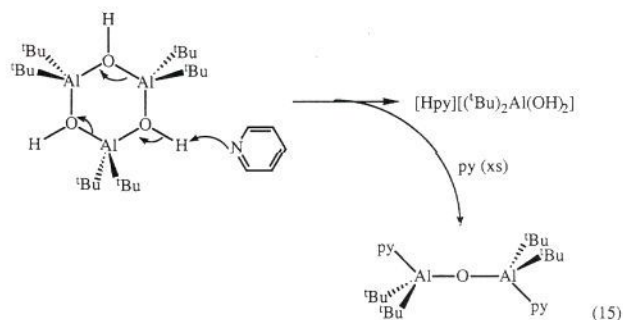
The molecular structure of $[(^t\text{Bu})_2\text{Al}(\text{py})]_2(\mu\text{-O})$ is shown in Figure 10; selected bond lengths and angles are given in Table VI. The molecule exists as a centrosymmetric dimer consisting of two $(^t\text{Bu})_2\text{Al}(\text{py})$ moieties linked by a single oxygen atom bridge such that the pyridine ligands are in a staggered *anti*-conformation. Although the Al–O–Al angle is 180° due to crystallographic symmetry, there appears to be no evidence of disorder, such as elongated thermal ellipsoids for, or significant residual electron density about, either the aluminum or the oxygen. The Al–O distance [1.710(1) Å] is comparable to those found for oxo-bridged complexes containing two five-coordinate aluminum atoms [1.679(2)–1.713(5) Å], in which the Al–O–Al angle varies between $152.0(3)^\circ$ and 180° .^{23–25} The infrared spectrum of **8** shows a strong asymmetric Al–O stretch at 973 cm^{-1} . This is consistent with a linear Al_2O linkage by comparison to the stretches observed for structurally characterized compounds $[\text{L}_2\text{Al}]_2(\mu\text{-O})$, $\text{L} = 2\text{-methyl-8-quinolinolato}$ (997 cm^{-1}),²³ $\text{L}_2 = \text{phthalocyaninato}$ (1051 cm^{-1}),²⁴ or N,N' -ethylenebis(salicylideneimine) (1067 cm^{-1}).²⁵

(56) Arif, A. M.; Barron, A. R. *Polyhedron* **1988**, *7*, 2091.

Pasynkiewicz and co-workers have reported that the partial hydrolysis of AlMe_3 in the presence of N,N,N',N' -tetramethylethylenediamine (TMEDA) gave the tetramethylalumoxane (**XII**) in low yield; however, no structural information was obtained.⁵⁷ Thus, while an example of a Lewis base complex of a tetraalkyldialuminumalumoxane has been characterized by NMR and mass spectral data,¹⁹ compound **8** represents the first example to be structurally characterized.



The formation of **8** from **1** is an interesting transformation. While we have no direct evidence for the mechanism and have been unable to isolate the coproducts, one possibility that is consistent with precedent⁵⁸ is that the initial reaction is probably deprotonation of one of the hydroxide ligands followed by disproportionation and subsequent pyridine coordination of the coordinatively unsaturated $[(^t\text{Bu})_2\text{Al}]_2(\mu\text{-O})$ fragment (eq 15).



As noted above, both compound **8** and $\text{Al}(^t\text{Bu})_3(\text{py})$ (**9**) are bright yellow in color. The UV/visible spectra of compounds **8** and **9** show, in addition to the expected $\pi\text{-}\pi^*$ bands for the pyridine ligand (**8**, 222 and 252 nm; **9**, 222 and 254 nm), low-energy absorptions at 340 and 344 nm in **8** and **9**, respectively. On the basis of literature precedent, we assign these bands to a ligand-to-ligand charge transfer from the electron-rich aluminum–alkyl σ bonds to the low-lying π^* orbital of the 6 π -electron heterocycle.⁵⁹

Structural Relationship of $[(^t\text{Bu})\text{Al}(\mu_3\text{-O})]_n$ ($n = 6, 8, 9$) and $[(^t\text{Bu})_2\text{Al}\{\mu\text{-OAl}(^t\text{Bu})_2\}]_2$ to Methylalumoxane. As outlined above, we have prepared and crystallographically characterized a number of *tert*-butylalumoxanes. While the isolation and structural elucidation of the *tert*-butylalumoxanes is an important advance in the chemistry of alkylalumoxanes per se, their relevance to the catalytically active species present in MAO has yet to be determined conclusively.⁶⁰ We believe, however, that the *tert*-butylalumoxanes do represent the first important step in the structural elucidation of MAO.

Before discussing similarities between our *tert*-butylalumoxanes and commercial MAO, we readily accept that there are a number of important differences between the ligating ability of the *tert*-butyl versus methyl alkyl groups, which may alter structure and reactivity. These differences include the relative steric bulk of *tert*-butyl versus methyl substituents as defined by their cone angles (126° versus 90°),⁵⁴ and the ability of the methyl group

(57) Sadownik, A.; Pasynkiewicz, S.; Boleslawski, M.; Szachnowska, H. *J. Organomet. Chem.* **1978**, *152*, C49.

(58) Leman, J. T.; Roman, H. A.; Barron, A. R. *J. Chem. Soc., Dalton Trans.* **1992**, 2183.

(59) See for example: (a) Baumgarten, J.; Bessenbacher, C.; Kaim, W.; Stahl, T. *J. Am. Chem. Soc.* **1989**, *111*, 2126. (b) Lichtenberger, D. L.; Hogan, R. H.; Healy, M. D.; Barron, A. R. *Organometallics* **1991**, *10*, 609.

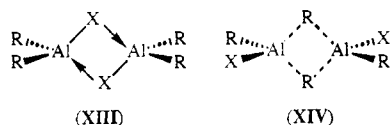
(60) Initial data indicates that the *tert*-butylalumoxanes are themselves active cocatalysts for a number of catalytic systems.

Table VI. Selected Bond Lengths (Å) and Angles (deg) for [(*t*-Bu)₂Al(py)]₂(μ-O) (**8**)

Al(1)–O(1)	1.710(1)	Al(1)–C(1)	2.020(3)
Al(1)–C(5)	2.017(3)	Al(1)–N(1)	2.029(2)
O(1)–Al(1a)	1.710(1)		
O(1)–Al(1)–C(1)	114.4(1)	O(1)–Al(1)–C(5)	113.5(1)
O(1)–Al(1)–N(1)	101.7(1)	C(1)–Al(1)–C(5)	117.0(1)
C(1)–Al(1)–N(1)	103.3(1)	C(5)–Al(1)–N(1)	104.6(1)
Al(1)–O(1)–Al(1a)	180.0(1)		

to act as a stable bridging ligand. Changes in steric bulk of substituents are often cited as the controlling factor in the magnitude of oligomerization. However, Kaminsky and Shilov⁶¹ have, on the basis of mass spectrometry and cryoscopy, reported that MAO consists of a range of hydrocarbon soluble species containing 5–12 aluminum atoms. We have isolated or spectroscopically characterized *tert*-butylaluminum species containing 4–12 aluminums. Hence, concerns that the *tert*-butyl group would as a consequence of steric bulk preclude oligomeric forms open to MAO are unfounded.

The second dissimilarity between methyl and *tert*-butyl substituents, the ability of the former to act as a bridging ligand,⁶² does mean that it is possible that some structural types present in MAO will not be formed with *tert*-butyl ligation. However, through a series of elegant NMR experiments, Mole demonstrated that the three-center four-electron bridge formed by group 15, 16, or 17 donor atoms (XIII) is always preferred to the possible formation of a three-center two-electron methyl bridge (XIV).⁶³ Thus, in the present case an oxo bridge will always be preferred over an alkyl bridge.



The solution ¹H and ¹³C NMR spectra of MAO show broad resonances consistent with a fluxional species. Similarly, the solid state ¹³C CPMAS NMR spectrum of MAO exhibits a single resonance sufficiently broad (δ –6.5, *W*_{1/2} ca. 750 Hz) to preclude assignment of specific Al–Me environments.^{11a} Aside from confirming the presence of aluminum-bound methyl groups, these ¹H and ¹³C NMR spectra do not provide any additional structural data. We have encountered similar problems with the structural assignment of the hydrolytically stable siloxy-substituted alumoxanes.³¹ In contrast, ²⁷Al and ¹⁷O NMR spectroscopic data are useful in defining possible (and precluding unlikely) coordination geometries of aluminum and oxygen in structurally unknown compounds. In this regard the heteroatom NMR chemical shifts of MAO, compounds 1–9, and related compounds are given in Table I.

The ²⁷Al NMR spectra of MAO (both a commercial sample and that prepared in our laboratory, see Experimental Section) and isobutylalumoxane (see Experimental Section) consist of single broad resonances (δ 149–152). Thus, on the basis of ²⁷Al NMR spectroscopy, it is difficult to preclude the presence of aluminum centers in three-coordinate R₂AlO or four-coordinate R₂AlO₂ coordination environments in addition to the RAlO₃ environments observed for [(*t*-Bu)Al(μ₃-O)]_n (*n* = 6, 8, 9). However, we can reasonably preclude as a major contributor, a three-coordinate RAlO₂ environment present in the cyclic structures previously proposed,¹⁹ since this should appear at 100

(61) Grogorjan, E. A.; Dyachkovskii, F. S.; Shilov, A. E. *Vysokomol. Soedin.* **1965**, *7*, 145.

(62) We note that although there are no examples of isolable group 13 compounds with *tert*-butyl bridging ligation, the observation of ligand-exchange reactions implies their existence albeit as transition states, see: Cleaver, W. M.; Barron, A. R. *Chemtronics* **1989**, *4*, 146.

(63) (a) Jeffery, E. A.; Mole, T.; Saunders, J. K. *Can. J. Chem.* **1968**, *21*, 137. (b) Jeffery, E. A.; Mole, T.; Saunders, J. K. *Can. J. Chem.* **1968**, *21*, 649.

ppm.⁴⁴ In addition, it is worth noting that while, on the basis of ¹H and ¹³C NMR spectroscopy and X-ray crystallography, two chemically distinct aluminum sites are present in the iminoalane [HAL(μ₃-NEt)]_n,⁶⁴ only a single broad resonance is observed in the ²⁷Al NMR spectrum (δ 158).

The ¹⁷O NMR spectrum of MAO consists of a single broad (*W*_{1/2} = 800 Hz) resonance at 55 ppm. This resonance is within the range observed for either a three-coordinate oxo ligand (δ 55–75) or three-coordinate hydroxide moiety (δ 54) structurally characterized in compounds **2**, **4**, and **5**, and Al₁₀(OH)₁₆(OSiEt₃)₁₄,³¹ respectively. Since the hydroxide groups may be rejected as contributing significantly to the structure of MAO on the basis of IR and ¹H NMR spectroscopy, the oxo ligands in MAO are clearly trifurcated. At the present time, insufficient data are available to determine the geometry, planar versus tetrahedral, of the oxide due to overlapping of the regions (see Table I). The absence of two-coordinate oxo ligands, Al(μ-O)Al, is suggested by the absence of any resonance close to that observed for **8** (δ 17) in the ¹⁷O NMR spectrum.

Conclusion

We have determined that alkylalumoxanes prepared by the equimolar hydrolysis of Al(*t*-Bu)₃ have the general formula [(*t*-Bu)Al(μ₃-O)]_n. Partial hydrolysis results in the formation of the tetraaluminum compound [(*t*-Bu)₂Al{μ-OAl(*t*-Bu)₂}]₂. On the basis of spectroscopic evidence and with the assistance of X-ray structural characterization, we have proposed that MAO and related alkylalumoxanes, (RAIO)_n, have cluster structures analogous to those found for the iminoalanes, in which the aluminum centers are four-coordinate. Furthermore, we have proposed that this oxygen coordination environment involves bridging three aluminum atoms. We are at present investigating the reactivity and catalytic activity of the *tert*-butylalumoxanes, and the results will be presented elsewhere.

Experimental Section

Melting points were determined in sealed capillaries and are uncorrected. Mass spectra were obtained on a JEOL AX-505 H mass spectrometer operating with an electron beam energy of 70 eV for EI mass spectra. Ammonia was used as the reagent gas for CI experiments unless otherwise indicated. Infrared spectra (4000–400 cm⁻¹) were obtained using a Nicolet 5ZDX-FTIR spectrometer. IR samples were prepared as mulls on KBr plates. NMR spectra were obtained on Bruker AM-400 (¹H, ¹³C) or Bruker WM-300 (¹⁷O, ²⁷Al) spectrometers using (unless otherwise stated) benzene-*d*₆ solutions. Variable-temperature ¹H NMR spectra were obtained on a Bruker AM-500 spectrometer. Chemical shifts are reported relative to external TMS (¹H, ¹³C), H₂O (¹⁷O), or aqueous [Al(H₂O)₆]³⁺ (²⁷Al). Samples for ¹⁷O NMR experiments were prepared using 20.4% H₂¹⁷O-enriched water in the syntheses described below. ²⁷Al and ¹⁷O NMR data are given in Table I. Microanalyses were performed by Oneida Research Services, Inc., Whitesboro, New York.

All procedures were performed under purified nitrogen. Solvents were distilled and degassed prior to use. A commercial sample of methylalumoxane was obtained from Akzo Chemicals, Inc. Volatiles were removed in vacuo, and the remaining solid was redissolved in benzene-*d*₆ for spectroscopic measurements. Al(*t*-Bu)₃ was prepared as previously reported.³⁸

[(*t*-Bu)₂Al(μ-OH)]₃ (**1**). H₂O (0.97 mL, 54 mmol) was injected into a cooled (–78 °C) solution of Al(*t*-Bu)₃ (10.0 g, 50.4 mmol) in pentane (300 mL). After being stirred for 1.5 h, the reaction mixture was allowed to warm to room temperature and the resulting solution was stirred an additional 2 h. Cooling (–20 °C) overnight yielded clear crystals, which were isolated by filtration and dried in vacuo. The filtrate was concentrated in vacuo and cooled overnight to afford a second crop of product. Combined yield 2.96 g, 35%. Anal. Calcd for C₉H₁₉AlO: C, 60.73; H, 12.10. Found: C, 58.68; H, 11.75. MS (CI, isobutane, %) *m/z*: 475 (3M⁺ + H, 5), 417 (3M⁺ – *t*-Bu, 100). IR (cm⁻¹): 3584 (s, ν_{OH}), 1362 (m), 1043 (s), 998 (m), 936 (w), 815 (m), 635 (s), 506 (w). ¹H NMR: δ 2.02 (1H, s, OH), 1.10 [18H, s, C(CH₃)₃]. ¹³C NMR: δ 31.14 [C(CH₃)₃].

(64) Noth, H.; Wolfgardt, P. Z. *Naturforsch.* **1976**, *B31*, 697.

Synthesis of $[(^i\text{Bu})_2\text{Al}(\mu\text{-OAl}(^i\text{Bu})_2)]_2$ (2) and $[(^i\text{Bu})\text{Al}(\mu_3\text{-O})]_6$ (3). A solution of $\text{Al}(^i\text{Bu})_3$ (15.0 g, 75.6 mmol) in toluene (75 mL) was added to a cooled (-78°C) suspension of $\text{Al}_2(\text{SO}_4)_3 \cdot 18\text{H}_2\text{O}$ (2.84 g, 76.7 mmol of H_2O) in toluene (150 mL) over a period of 5 min. The mixture was stirred at -78°C for 1 h and was then allowed to warm to room temperature. Stirring was continued at room temperature for 2 h. The mixture was refluxed for 15 h, cooled, and filtered through Celite. The Celite was washed with fresh toluene (50 mL). The filtrate was concentrated *in vacuo* to approximately one third its original volume and was stored at -20°C for 2 days. A white crystalline product (1.95 g) was isolated by filtration and dried *in vacuo*. ^1H NMR revealed the presence of both compounds 2 and 3 in this product in a ratio of 3:1. Fractional crystallization from toluene (-20°C) yielded rod-like crystals of the less soluble 2 followed by needles of compound 3. The ^1H NMR spectrum of the remaining material from this reaction revealed a complex mixture. The presence of compounds 4 and 5 as minor components in this mixture was verified by ^1H NMR spectroscopy.

$[(^i\text{Bu})_2\text{Al}(\mu\text{-OAl}(^i\text{Bu})_2)]_2$ (2). MS (EI, %) m/z : 539 ($\text{M}^+ - ^i\text{Bu}$, 100), 483 ($\text{M}^+ - ^i\text{Bu} - \text{C}_4\text{H}_8$, 5), 425 ($\text{M}^+ - 3^i\text{Bu}$, 10). IR (cm^{-1}): 1364 (m), 1005 (w), 936 (w), 806 (s), 744 (vs), 601 (vs). ^1H NMR: δ 1.174 [36H, s, $\text{C}(\text{CH}_3)_3$], 1.169 [36H, s, $\text{C}(\text{CH}_3)_3$]. ^{13}C NMR: δ 32.14 [$\text{C}(\text{CH}_3)_3$], 30.86 [$\text{C}(\text{CH}_3)_3$].

$[(^i\text{Bu})\text{Al}(\mu_3\text{-O})]_6$ (3). MS (EI, %) m/z : 800 ($8\text{M}^+ - 7$), 743 ($8\text{M}^+ - ^i\text{Bu}$, 100), 687 ($8\text{M}^+ - ^i\text{Bu} - \text{C}_4\text{H}_8$, 10). MS (CI, %) m/z : 818 ($\text{M}^+ + \text{NH}_4$, 100), 760 ($\text{M}^+ + \text{NH}_4 - ^i\text{Bu}$, 25). ^1H NMR: δ 1.23 [36H, s, $\text{C}(\text{CH}_3)_3$], 1.18 [36H, s, $\text{C}(\text{CH}_3)_3$]. ^{13}C NMR: δ 29.74, 29.07 [$\text{C}(\text{CH}_3)_3$].

Synthesis of $[(^i\text{Bu})\text{Al}(\mu_3\text{-O})]_6$ (4) and $[(^i\text{Bu})\text{Al}(\mu_3\text{-O})]_9$ (5). Freshly prepared $[(^i\text{Bu})_2\text{Al}(\mu_2\text{-OH})]_3$ (1.50 g, 3.16 mmol) was refluxed in hexane (150 mL), for 24 h to give a clear solution. Heating was discontinued, and the volatiles were removed *in vacuo* to leave a white powder. Toluene (15 mL) was added and the resulting solution filtered to remove traces of insoluble material. The clear solution was cooled overnight at -20°C to yield long colorless needles of the hexamer (4), which were isolated by filtration and dried *in vacuo*. The filtrate was concentrated and cooled at -20°C for several days to yield rod-like crystals of the nonamer (5).

$[(^i\text{Bu})\text{Al}(\mu_3\text{-O})]_6$ (4). MS (EI, %) m/z : 600 (6M^+ , 40), 543 ($6\text{M}^+ - ^i\text{Bu}$, 100). IR (cm^{-1}): 1005 (w), 938 (w), 818 (sh), 795 (vs), 619 (m), 579 (m), 562 (m). ^1H NMR: δ 1.16 [s, $\text{C}(\text{CH}_3)_3$]. ^{13}C NMR: δ 28.7 [$\text{C}(\text{CH}_3)_3$].

$[(^i\text{Bu})\text{Al}(\mu_3\text{-O})]_9$ (5). MS (EI, %) m/z : 900 (9M^+ , 30), 843 ($9\text{M}^+ - ^i\text{Bu}$, 100). IR (cm^{-1}): 832 (s), 817 (s), 775 (m), 744 (s), 676 (s), 627 (m), 563 (m), 449 (m). ^1H NMR: δ 1.22 [27H, s, $\text{C}(\text{CH}_3)_3$], 1.21 [54H, s, $\text{C}(\text{CH}_3)_3$]. ^{13}C NMR: δ 30.22 [18C, s, $\text{C}(\text{CH}_3)_3$], 29.87 [9C, s, $\text{C}(\text{CH}_3)_3$].

$[(^i\text{Bu})_2\text{Al}(\mu\text{-OH})]_3 \cdot 2\text{THF}$ (6). Excess THF (0.5 mL) was added to a suspension of $[(^i\text{Bu})_2\text{Al}(\mu\text{-OH})]_3$ (1.00 g, 2.11 mmol) in pentane (25 mL) to give a clear solution. The solution was cooled (-20°C) overnight to yield clear crystals. Further product was obtained by concentrating the filtrate *in vacuo* and cooling overnight. The yield was essentially quantitative. IR (cm^{-1}): 3690 (s, ν_{OH}), 3160 (m, ν_{OH}), 1189 (s), 1044 (s), 1003 (s), 935 (m), 919 (m), 842 (s), 815 (s), 725 (s). ^1H NMR: δ 3.51 (8H, m, OCH_2 , THF), 3.42 (3H, s, OH), 1.31 (8H, m, OCH_2CH_2 , THF), 1.19 [54H, s, $\text{C}(\text{CH}_3)_3$]. ^{13}C NMR: δ 68.5 (OCH_2CH_2), 31.5 [$\text{C}(\text{CH}_3)_3$], 25.2 (OCH_2CH_2), 15.8 [broad, $\text{C}(\text{CH}_3)_3$].

$[(^i\text{Bu})_2\text{Al}(\mu\text{-OH})]_3 \cdot 2\text{MeCN}$ (7). Dissolution of $[(^i\text{Bu})_2\text{Al}(\mu\text{-OH})]_3$ (0.35 g, 0.74 mmol) in acetonitrile (15 mL) gave a clear solution. The volatiles were removed *in vacuo* to leave the pure product as a white powder in essentially quantitative yield. The product may be crystallized from pentane or methylene chloride solutions containing acetonitrile. IR (cm^{-1}): 3594 (m, ν_{OH}), 3260 (broad, vs, ν_{OH}), 2265 (m, ν_{CN}), 1360 (m), 1192 (s), 1177 (sh), 1037 (s), 1002 (m), 935 (w), 831 (sh), 815 (s), 775 (w), 744 (w), 667 (s), 649 (s). ^1H NMR: δ 3.90 (3H, s, OH), 1.33 [54H, s, $\text{C}(\text{CH}_3)_3$], 0.46 (6H, s, CH_3CN). ^{13}C NMR: δ 116.6 (CH_3CN), 31.6 [$\text{C}(\text{CH}_3)_3$], 15.8 [b s, $\text{C}(\text{CH}_3)_3$], -0.30 (CH_3CN).

$[(^i\text{Bu})_2\text{Al}(\text{py})_2(\mu\text{-O})]$ (8). Method 1. $[(^i\text{Bu})_2\text{Al}(\mu\text{-OH})]_3$ (0.60 g, 1.26 mmol) was added to pyridine (25 mL) to give a bright-yellow solution. Refluxing the solution overnight resulted in no visible change. The solvent was removed *in vacuo* to leave a light-yellow powder, which was recrystallized from hot toluene/hexane to yield large yellow crystals. Yield 0.49 g, 57%.

Method 2. H_2O (50 μL , 2.8 mmol) was injected into a cooled (-40°C) solution of $\text{Al}(^i\text{Bu})_3$ (1.05 g, 5.29 mmol) in pyridine (35 mL). The resulting light-yellow solution was allowed to warm to room temperature with stirring for 2 h and then refluxed for 2 h. The volume of the solution was reduced to approximately 5 mL *in vacuo*. Hexane (10 mL) was added, and the resulting mixture was heated mildly to give a yellow

solution which was cooled at -20°C overnight to yield yellow crystals of the product. Yield 0.54 g, 45%.

Method 3. Pyridine (ca. 0.20 mL) was added to an NMR tube containing a solution of $[(^i\text{Bu})_2\text{Al}(\mu\text{-OAl}(^i\text{Bu})_2)]_2$ (0.025 g, 0.042 mmol) in C_6D_6 . Over the course of 2 h this clear solution became yellow. ^1H NMR spectroscopy verified complete conversion of the starting material to $[(^i\text{Bu})_2\text{Al}(\text{py})_2(\mu_2\text{-O})]$. MS (EI, %) m/z : 320 ($\text{M}^+ - \text{py} - ^i\text{Bu}$, 70), 298 ($\text{M}^+ - 2\text{py}$, 35), 241 ($\text{M}^+ - 2\text{py} - ^i\text{Bu}$, 70), 185 ($\text{M}^+ - 2\text{py} - 2^i\text{Bu}$, 100). MS (CI, NH_3 , %) m/z : 416 ($\text{M}^+ + \text{NH}_3 - ^i\text{Bu}$, 15), 333 ($\text{M}^+ + \text{H} - 2\text{py} + 2\text{NH}_3$, 100). IR (cm^{-1}): 1611 (s), 1487 (w), 1452 (vs), 1213 (w), 1070 (m), 1047 (s), 1018 (w), 999 (m), 973 (vs, $\nu(\text{as})_{\text{AlO}}$), 934 (m), 812 (s), 760 (m), 700 (s), 645 (m), 575 (s), 529 (w), 416 (m). UV/vis (CH_2Cl_2 , nm): 222 ($\epsilon = 2300 \text{ M}^{-1} \text{ cm}^{-1}$), 252 ($\epsilon = 3500 \text{ M}^{-1} \text{ cm}^{-1}$), 340 ($\epsilon = 1000 \text{ M}^{-1} \text{ cm}^{-1}$). ^1H NMR: δ 8.89 (2H, d, *o*-CH, py), 6.75 (1H, t, *p*-CH, py), 6.52 (2H, t, *m*-CH, py), 1.38 [18H, s, $\text{C}(\text{CH}_3)_3$]. ^{13}C NMR: δ 147.8 (*o*-CH, py), 139.8 (*p*-CH, py), 124.3 (*m*-CH, py), 32.4 [$\text{C}(\text{CH}_3)_3$].

$\text{Al}(^i\text{Bu})_3(\text{py})$ (9). To a cold (-78°C) pentane solution (40 mL) of $\text{Al}(^i\text{Bu})_3$ (1.32 g, 6.66 mmol) was added pyridine (~ 1.5 mL) to yield a yellow solution. The solution was warmed to room temperature, and the volatiles were removed *in vacuo* to leave pure product in quantitative yield. The yellow solid readily sublimates under reduced pressure (0.01 Torr) at a bath temperature of 100°C . MS (EI, %) m/z : 276 ($\text{M}^+ - \text{H}$, 5), 220 ($\text{M}^+ - ^i\text{Bu}$, 30), 198 ($\text{M}^+ - \text{py}$, 50), 141 ($\text{M}^+ - \text{py} - ^i\text{Bu}$, 100). UV/vis (pentane, nm): 222 ($\epsilon = 3500 \text{ M}^{-1} \text{ cm}^{-1}$), 254 ($\epsilon = 3000 \text{ M}^{-1} \text{ cm}^{-1}$), 344 ($\epsilon = 1100 \text{ M}^{-1} \text{ cm}^{-1}$). ^1H NMR: δ 8.46 (2H, d, *o*-CH, py), 6.65 (1H, t, *p*-CH, py), 6.32 (2H, t, *m*-CH, py), 1.32 [27H, s, $\text{C}(\text{CH}_3)_3$]. ^{13}C NMR: δ 147.9 (*o*-CH, py), 139.8 (*p*-CH, py), 124.6 (*m*-CH, py), 33.0 [$\text{C}(\text{CH}_3)_3$], 17.0 [$\text{C}(\text{CH}_3)_3$].

Hydrolysis of AlMe_3 . H_2O (30 μL , 1.7 mmol) was injected into a cooled (-78°C) solution of AlMe_3 (1.0 mL of 2.0 M solution in toluene, 2.0 mmol) in toluene- d_8 . The solution was slowly warmed to room temperature over a period of 1 h. Stirring was continued for 2 h at room temperature. The resulting sample was transferred to a 10-mm NMR tube for spectroscopic characterization. CAUTION: The hydrolysis of AlMe_3 is vigorous with the evolution of heat and methane.

Hydrolysis of $\text{Al}(^i\text{Bu})_3$. A solution of $\text{Al}(^i\text{Bu})_3$ (2.0 mL of 1.0 M solution in hexane, 2.0 mmol) in toluene- d_8 (2.0 mL) was hydrolyzed with H_2O (30 μL , 1.7 mmol) as described above. In addition, the sample was heated at 50°C for 2 h to ensure complete reaction. The resulting solution was transferred to a 10-mm NMR tube for spectroscopic characterization.

Crystallographic Studies. Crystals of compounds 1, 6, 7, and 8 were mounted directly onto a glass pin attached to the goniometer head with silicon grease. X-ray data were collected on a Nicolet R3m/V four-circle diffractometer equipped with an LT-1 low-temperature device. Data collection using the Nicolet P3 program unit cell and space group determination were all carried out in a manner previously described in detail.⁶⁵ A semiempirical absorption correction and Lorentz and polarization corrections were applied to all data. The structures of compounds 1, 6, 7, and 8 were solved using the direct methods program XS,⁶⁶ which readily revealed the positions of the Al, O, and N (7, 8) and the majority of the C atoms. Subsequent difference Fourier maps eventually revealed the positions of all of the non-hydrogen atoms for all structures. After all of the non-hydrogen atoms were located and refined anisotropically, the difference map either revealed some (6, 7, and 8) or all (1) of the hydrogen atom positions. For 1 it was possible to identify and successfully refine all organic hydrogens. Organic hydrogen atoms for 6, 7, and 8 were placed in calculated positions $\{U_{\text{iso}}(\text{H}) = 1.2[U_{\text{iso}}(\text{C})]; d(\text{C}-\text{H}) = 0.96 \text{ \AA}\}$ for refinement. All hydrogen atoms were fixed in the final refinement. Neutral-atom scattering factors were taken from the usual source.⁶⁷ Refinement of positional and anisotropic thermal parameters led to convergence (see Table VII). Final atomic positional parameters are given in Tables VIII and XI–XIII.

A suitable colorless block crystal of compound 2 was sealed inside a Lindemann capillary and mounted on the goniometer of an Enraf-Nonius CAD-4 diffractometer employing $\text{Mo K}\alpha$ radiation ($\lambda = 0.71073 \text{ \AA}$). The diffractometer was configured with a crystal-to-detector distance of 173 nm and a takeoff angle of 2.80° . After the crystal was carefully centered in the X-ray beam, an automatic search routine was used to locate up to 25 reflections, which were subsequently used to calculate a preliminary cell. After analysis of this initial cell showed no higher

(65) Healy, M. D.; Wierda, D. A.; Barron, A. R. *Organometallics* 1988, 7, 2543.

(66) Nicolet Instruments Corporation, Madison, WI, 1988.

(67) *International Tables for X-Ray Crystallography*; Kynoch Press: Birmingham, England, 1974; Vol. 4.

Table VII. Summary of X-ray Diffraction Data

compound	$[(\text{Bu})_2\text{Al}(\mu\text{-OH})]_3$ (1)	$[(\text{Bu})_2\text{Al}(\mu\text{-O})]_6$ (4)	$[(\text{Bu})_2\text{Al}(\mu\text{-OH})]_3$ (6)	$[(\text{Bu})_2\text{Al}(\mu\text{-OH})]_3$ (7)	$[(\text{Bu})_2\text{Al}(\mu\text{-OH})]_3$ (8)
emp form	$\text{C}_{24}\text{H}_{57}\text{Al}_3\text{O}_3$	$\text{C}_{24}\text{H}_{54}\text{Al}_6\text{O}_6$	$\text{C}_{32}\text{H}_{73}\text{Al}_3\text{O}_5$	$\text{C}_{28}\text{H}_{63}\text{Al}_3\text{N}_2\text{O}_3$	$\text{C}_{24}\text{H}_{46}\text{Al}_2\text{N}_2\text{O}$
cryst size, mm	$0.31 \times 0.35 \times 0.31$	see text	$0.35 \times 0.30 \times 0.23$	$0.40 \times 0.48 \times 0.40$	$0.40 \times 0.48 \times 0.31$
cryst syst	monoclinic	triclinic	monoclinic	monoclinic	triclinic
space group	$C2/c$	$P1$	$P2_1/c$	$P2_1/n$	$P1$
<i>a</i> , Å	17.697(3)	11.847(3)	11.463(3)	11.406(2)	9.074(2)
<i>b</i> , Å	10.198(6)	12.208(2)	15.603(6)	21.297(7)	9.486(3)
<i>c</i> , Å	17.781(5)	13.711(4)	22.263(6)	14.972(2)	9.728(3)
α , deg	109.37(2)	103.83(2)	95.63(2)	96.76(2)	104.28(2)
β , deg	3026(2)	109.02(1)	92.37(3)	112.92(2)	99.48(2)
γ , deg	4	1805(3)	3963	714.8(3)	112.92(2)
<i>V</i> , Å ³	1.042	2	4	1	1
<i>Z</i>	0.145	1.005	1.037	1.061	1.061
<i>D</i> (calcd), g/cm ³	193	1.369	0.127	0.131	0.120
μ , mm ⁻¹	4.0–50.0	2.0–40.0	4.0–50.0	4.0–45.0	4.0–45.0
radiation	2θ range, deg	2θ range, deg	2θ range, deg	2θ range, deg	2θ range, deg
temp, K	no. collected	no. collected	no. collected	no. collected	no. collected
no. obsd	no. ind	no. ind	no. ind	no. ind	no. ind
no. obsd	no. obsd	no. obsd	no. obsd	no. obsd	no. obsd
weighting scheme	$w^{-1} = \sigma^2(F_o) + 0.0014(F_o)^2$	$w^{-1} = \sigma^2(F_o) + 0.04(F_o)^2$	$w^{-1} = \sigma^2(F_o) + 0.0010(F_o)^2$	$w^{-1} = \sigma^2(F_o) + 0.0006(F_o)^2$	$w^{-1} = \sigma^2(F_o)$
<i>R</i>	0.0481	0.0689	0.0550	0.0381	0.0424
<i>R_w</i>	0.0587	0.0972	0.0757	0.0408	0.0453
largest diff peak, eÅ ⁻³	0.21	0.57	0.28	0.21	0.26

Table VIII. Atomic Coordinates ($\times 10^4$) and Equivalent Isotropic Thermal Parameters ($\text{\AA}^2 \times 10^3$) for $[(\text{Bu})_2\text{Al}(\mu\text{-OH})]_3$ (1)

	<i>x</i>	<i>y</i>	<i>z</i>	<i>U</i> (eq) ^a
Al(1)	0	523(1)	2500	18(1)
O(1)	787(2)	1710(2)	2497(2)	30(1)
Al(2)	989(1)	3489(1)	2500(1)	17(1)
O(2)	0	4081(3)	2500	29(2)
C(11)	316(3)	-484(3)	3520(2)	23(2)
C(12)	840(3)	313(3)	4239(3)	36(2)
C(13)	-434(3)	-934(4)	3683(3)	31(2)
C(14)	815(3)	-1716(4)	3477(3)	36(2)
C(21)	1832(3)	3962(3)	3521(3)	23(2)
C(22)	1551(3)	3971(4)	4242(3)	34(2)
C(23)	2525(3)	2966(3)	3677(3)	34(2)
C(24)	2200(3)	5334(3)	3489(3)	33(2)
C(25)	1142(3)	4013(3)	1481(3)	24(2)
C(26)	625(3)	3222(2)	756(3)	36(2)
C(27)	893(3)	5463(3)	1312(3)	30(2)
C(28)	2017(3)	3883(4)	1518(3)	33(2)

^a Equivalent isotropic *U* defined as $1/3$ rd the trace of the orthogonalized U_{ij} tensor.

Table IX. Atomic Coordinates and Equivalent Isotropic Thermal Parameters ($\text{\AA}^2 \times 10^2$) for $[(\text{Bu})_2\text{Al}(\mu\text{-OAl}(\text{Bu})_2)]_2$ (2)^a

	<i>x</i>	<i>y</i>	<i>z</i>	<i>U</i> (eq)
Al(1)	0.09944(4)	0.1667(2)	0.54401(7)	2.67(3)
Al(2)	0.14807(4)	0.2237(2)	0.47309(7)	2.41(3)
Al(3)	0.17297(4)	0.2007(2)	0.62813(8)	3.20(4)
Al(4)	0.07466(4)	0.1867(2)	0.38859(8)	3.31(4)
O(1)	0.14438(7)	0.1974(4)	0.5582(2)	2.36(7)
O(2)	0.10323(7)	0.1932(4)	0.4584(2)	2.52(7)
C(11)	0.0633(1)	0.3109(7)	0.5543(3)	3.8(1)
C(12)	0.0525(2)	0.3169(9)	0.6197(3)	6.1(2)
C(13)	0.0697(2)	0.4682(8)	0.5349(3)	5.3(2)
C(14)	0.0341(1)	0.2536(8)	0.5070(3)	5.2(2)
C(15)	0.0971(1)	-0.0259(6)	0.5914(3)	3.3(1)
C(16)	0.1175(2)	-0.1496(7)	0.5693(3)	4.5(2)
C(17)	0.0635(2)	-0.0898(8)	0.5945(3)	5.5(2)
C(18)	0.1119(2)	0.0113(8)	0.6593(3)	4.5(2)
C(21)	0.1719(1)	0.4186(6)	0.4766(3)	3.2(1)
C(22)	0.2045(1)	0.3866(8)	0.5209(3)	4.6(2)
C(23)	0.1550(2)	0.5410(7)	0.5080(3)	4.3(2)
C(24)	0.1805(2)	0.4805(7)	0.4148(3)	4.8(2)
C(25)	0.1626(1)	0.0761(6)	0.4118(2)	3.0(1)
C(26)	0.1453(2)	0.1253(7)	0.3470(3)	4.3(2)
C(27)	0.1522(2)	-0.0833(7)	0.4220(3)	4.5(2)
C(28)	0.1990(2)	0.0732(8)	0.4074(3)	5.3(2)
C(31)	0.2086(1)	0.0505(8)	0.6415(3)	4.3(2)
C(32)	0.2031(2)	-0.0669(9)	0.6902(4)	7.2(2)
C(33)	0.2407(2)	0.131(1)	0.6682(4)	6.8(2)
C(34)	0.2135(2)	-0.028(1)	0.5814(3)	6.9(2)
C(35)	0.1704(2)	0.3559(7)	0.6929(3)	4.6(2)
C(36)	0.1781(2)	0.287(1)	0.7595(3)	7.9(2)
C(37)	0.1956(2)	0.4797(9)	0.6899(4)	7.2(2)
C(38)	0.1373(2)	0.4298(9)	0.6870(3)	6.8(2)
C(41)	0.0654(1)	0.3666(7)	0.3354(3)	4.4(2)
C(42)	0.0628(2)	0.3258(9)	0.2643(3)	6.4(2)
C(43)	0.0913(2)	0.4854(8)	0.3500(3)	6.0(2)
C(44)	0.0329(2)	0.4392(9)	0.3443(4)	6.5(2)
C(45)	0.0511(2)	-0.0009(7)	0.3630(3)	4.1(1)
C(46)	0.0535(2)	-0.1152(9)	0.4151(3)	6.4(2)
C(47)	0.0627(2)	-0.0719(9)	0.3056(3)	6.0(2)
C(48)	0.0150(2)	0.038(1)	0.3419(4)	6.9(2)

^a Atoms denoted by asterisks were refined isotropically. Anisotropically refined atoms are given in the form of the isotropic equivalent displacement parameter defined as $4/3[a^2B_{(1,1)} + b^2B_{(2,2)} + c^2B_{(3,3)} + ab(\cos \gamma)B_{(1,2)} + ac(\cos \beta)B_{(1,3)} + bc(\cos \alpha)B_{(2,3)}]$.

symmetry of centering,⁶⁸ the cell parameters were refined on the basis of least-squares refinement of 25 reflections with $2\theta > 36^\circ$. Intensity data were collected using an ω scan technique with variable scan width $\Delta\omega = (0.80 + 0.35 \tan \theta)$. Backgrounds were measured by extending the calculated width on either end of the scan by 25%. A fixed vertical detector aperture (4 mm) and a variable horizontal detector aperture (3 + $\tan \theta$ mm) were used. Reflections with $I/\sigma(I) < 2$ for the prescan were

(68) *CAD4 Operations Manual*; Enraf-Nonius: Delft, The Netherlands, 1989.

Table X. Atomic Coordinates and Equivalent Isotropic Thermal Parameters ($\text{\AA} \times 10^2$) for $[(^t\text{Bu})\text{Al}(\mu_3\text{-O})]_6$ (4)^a

	x	y	z	U(eq)
Al(1)	0.1786(2)	0.4711(2)	0.5566(2)	2.83(6)
Al(2)	0.0684(2)	0.5702(2)	0.4036(2)	2.88(5)
Al(3)	-0.0143(2)	0.3273(2)	0.4238(2)	3.17(6)
Al(4)	0.5007(2)	0.9858(2)	0.8447(2)	3.11(6)
Al(5)	0.4006(2)	0.8472(2)	0.9778(2)	2.89(5)
Al(6)	0.6266(2)	0.8871(2)	0.9908(2)	2.95(6)
O(1)	0.0859(4)	0.4262(4)	0.4076(3)	2.6(1)*
O(2)	0.1412(4)	0.6116(4)	0.5535(3)	2.7(1)*
O(3)	0.0640(4)	0.3858(4)	0.5731(3)	2.8(1)*
O(4)	0.6445(4)	1.0215(4)	0.9644(4)	3.1(1)*
O(5)	0.5537(4)	0.8938(4)	1.0879(3)	2.9(1)*
O(6)	0.4739(4)	0.8597(4)	0.8838(3)	2.7(1)*
C(1)	0.3406(6)	0.4376(6)	0.6051(5)	2.9(2)*
C(2)	0.1276(7)	0.6288(7)	0.3092(6)	3.4(2)*
C(3)	-0.0235(7)	0.1654(7)	0.3543(7)	4.5(2)*
C(4)	0.5035(7)	0.9751(7)	0.7023(6)	3.7(2)*
C(5)	0.3056(7)	0.7025(7)	0.9566(6)	4.2(2)*
C(6)	0.7488(8)	0.7867(8)	0.9841(7)	5.6(2)*
C(11)	0.3638(8)	0.3531(9)	0.5108(8)	6.9(3)
C(12)	0.3667(9)	0.3849(9)	0.6972(9)	7.2(3)
C(13)	0.4306(8)	0.544(1)	0.639(1)	8.0(4)
C(21)	0.1193(9)	0.7557(9)	0.3213(9)	7.7(3)
C(22)	0.0579(8)	0.566(1)	0.1938(7)	6.9(3)
C(23)	0.2604(8)	0.614(1)	0.3306(8)	8.2(3)
C(31)	0.0426(8)	0.149(1)	0.2730(9)	8.3(3)
C(32)	-0.145(1)	0.107(1)	0.291(1)	14.5(6)
C(33)	0.034(2)	0.112(1)	0.437(1)	16.9(7)
C(41)	0.452(1)	0.870(1)	0.6254(9)	12.5(5)
C(42)	0.423(2)	1.052(1)	0.6489(9)	19.1(5)
C(43)	0.619(1)	1.010(2)	0.704(1)	20.1(8)
C(51)	0.2328(9)	0.6456(9)	0.8378(8)	7.0(3)
C(52)	0.398(1)	0.6244(9)	0.996(1)	12.8(5)
C(53)	0.214(1)	0.723(1)	1.0155(8)	14.3(4)
C(61)	0.874(2)	0.849(2)	1.065(2)	6.3(5)*
C(61A)	0.778(2)	0.738(2)	1.085(2)	8.7(7)*
C(62)	0.756(2)	0.759(2)	0.865(1)	5.6(5)*
C(62A)	0.875(2)	0.864(2)	0.997(2)	6.7(5)*
C(63)	0.711(2)	0.666(2)	0.991(2)	6.8(5)*
C(63A)	0.702(2)	0.684(2)	0.881(2)	10.1(8)*

^a Atoms denoted by asterisks were refined isotropically. Anisotropically refined atoms are given in the form of the isotropic equivalent displacement parameter defined as $\frac{1}{3}[a^2B_{(1,1)} + b^2B_{(2,2)} + c^2B_{(3,3)} + ab(\cos \gamma)B_{(1,2)} + ac(\cos \beta)B_{(1,3)} + bc(\cos \alpha)B_{(2,3)}]$.

rejected as weak, and those where $I/\sigma(I) > 10$ were accepted after the prescan. Reflections not falling into these two categories were rescanned at speeds ranging from 0.67 to 8.00 deg/min for up to 120 s in an attempt to increase $I/\sigma(I)$ to 10. Three reflections (-3,-1,2; -12,2,-2; -20,2,-2) were measured after every 3600 s of exposure time in order to monitor crystal decay (<1%). Crystal alignment was checked using the same reflections every 250 data points, and as their scattering vectors did not deviate by less than 0.10° from their calculated values throughout data collection, no recentering was required. 5276 reflections were collected between $2 < 2\theta < 44^\circ$, with index ranges $+h,+k,\pm l$, of which 5202 were unique ($R_{\text{merg}} = 0.029$).

The intensity (I) and standard deviation [$\sigma(I)$] for each reflection were calculated using eqs 16 and 17, respectively, where C is the total number

$$I = AS(C - 2B) \quad (16)$$

$$\sigma(I) = AS(C + 4B)^{1/2} \quad (17)$$

of integrated counts, B is the sum of the left and right backgrounds, A is an attenuator factor (14.3 or 1), and S is the scan rate. Observed structure factors and their standard deviations were calculated using eqs 18 and 19, where L_p is a Lorentz-polarization correction term and $p =$

$$F_o = (I/L_p)^{1/2} \quad (18)$$

$$\sigma(F_o) = \{[\sigma(I)]^2 + (pI)^2\}^{1/2}/L_p \quad (19)$$

0.04. An absorption correction was applied (DIFABS⁶⁹) but no correction was made for extinction.

(69) Walker, N.; Stuart, D. *Acta Crystallogr., Sect. A* 1983, 39, 159.

Table XI. Atomic Coordinates ($\times 10^4$) and Equivalent Isotropic Thermal Parameters ($\text{\AA} \times 10^3$) for $[(^t\text{Bu})_2\text{Al}(\mu\text{-OH})]_3 \cdot 2\text{THF}$ (6)

	x	y	z	U(eq) ^a
Al(1)	8092(1)	8392(1)	967(1)	25(1)
Al(2)	5085(1)	8016(1)	694(1)	24(1)
Al(3)	6767(1)	6801(1)	1746(1)	25(1)
O(1)	6555(2)	8474(2)	630(1)	28(1)
O(2)	5514(2)	7140(1)	1217(1)	24(1)
O(3)	7862(2)	7593(1)	1550(1)	26(1)
C(11)	8628(3)	9491(2)	1364(2)	30(1)
C(12)	8248(4)	10238(3)	939(2)	47(2)
C(13)	8114(4)	9660(3)	1961(2)	39(1)
C(14)	9975(4)	9527(3)	1489(2)	49(2)
C(15)	9013(3)	7959(3)	314(2)	32(1)
C(16)	8298(4)	7375(3)	-135(2)	51(2)
C(17)	9488(5)	8676(3)	-64(2)	61(2)
C(18)	10063(4)	7440(3)	597(2)	61(2)
C(21)	4124(3)	8902(2)	1066(2)	30(1)
C(22)	3478(4)	9502(3)	604(2)	52(2)
C(23)	4890(4)	9475(3)	1502(2)	48(2)
C(24)	3215(4)	8470(3)	1432(2)	47(2)
C(25)	4447(3)	7558(2)	-106(2)	29(1)
C(26)	4609(4)	8226(3)	-595(2)	50(2)
C(27)	5038(4)	6729(3)	-285(2)	40(2)
C(28)	3122(3)	7371(3)	-114(2)	46(2)
C(31)	6398(3)	6978(3)	2593(2)	33(1)
C(32)	5155(4)	6609(3)	2647(2)	46(2)
C(33)	7259(4)	6506(3)	3049(2)	46(2)
C(34)	6370(4)	7919(3)	2788(2)	50(2)
C(35)	7269(3)	5619(2)	1536(2)	33(1)
C(36)	7131(4)	5457(3)	855(2)	49(2)
C(37)	6578(4)	4908(3)	1822(2)	51(2)
C(38)	8572(4)	5504(3)	1761(2)	54(2)
O(4)	3747(2)	6938(2)	1177(1)	43(1)
C(41)	3583(4)	5186(3)	607(3)	52(2)
C(42)	2489(6)	4813(4)	931(4)	117(3)
C(43)	1938(5)	5340(4)	1344(3)	84(3)
C(44)	2750(4)	6019(3)	1513(3)	70(2)
O(5)	9672(2)	7656(2)	2460(1)	44(1)
C(51)	9818(4)	8120(3)	3019(2)	55(2)
C(52)	10901(4)	7747(3)	3362(2)	58(2)
C(53)	11628(4)	7496(3)	2863(2)	64(2)
C(54)	10733(4)	7198(3)	2375(2)	58(2)

^a Equivalent isotropic U defined as $1/3$ rd the trace of the orthogonalized U_{ij} tensor.

All computations were carried out on a DEC VAXStation 3100/76. Calculations, except where noted, were performed using the MolEN crystallographic software package.⁷⁰ The structure was solved using MULTAN,⁷¹ which revealed the positions of the Al and O atoms. All remaining non-hydrogen atoms were located using difference Fourier maps and least-squares refinement. All non-hydrogen atoms were refined with anisotropic thermal parameters. Hydrogen atoms were generated and allowed to ride on the appropriate carbon [$U(\text{H}) = 1.3U_{\text{eq}}(\text{C})$]. The function minimized during refinement was $\sum w(|F_o| - |F_c|)^2$ where $w = 1/(\sigma F)^2$. Final refinement based on 2680 unique reflections with $I > 3\sigma(I)$ converged at $R = 0.0479 = (\sum(|F_o| - |F_c|))/(\sum|F_o|)$ and $R_w = 0.0538 = [w\sum(|F_o| - |F_c|)^2/w\sum(|F_o|^2)]^{1/2}$. The standard deviation of an observation of unit weight = 0.88.

After the final cycle of least squares, the maximum shift of a parameter was less than 0.01 of its estimated standard deviation, and the final difference map showed no feature higher than 0.22 $e/\text{\AA}^3$, close to Al(4). Scattering factors were taken from Cromer and Weber,⁶⁷ and anomalous dispersion effects were included in F_c using the values of Cromer.⁶⁷ Plots of $\sum w(|F_o| - |F_c|)^2$ vs $|F_o|$, $\sin \theta$, or data collection order showed no unusual trends.

General procedures used for data collection of compound 4 were as for 2. Due to drastic crystal decay, however, three data crystals were utilized, measuring $0.22 \times 0.48 \times 0.53$ (a), $0.08 \times 0.21 \times 0.32$ (b), and $0.31 \times 0.68 \times 0.97$ (c) mm. All crystals were mounted in capillaries containing mother liquor (toluene solutions). Three standard reflections were used throughout data collection (-2,-1,4; -2,4,0; -4,-1,3), and

(70) MolEN, *An Interactive Structure Solution Program*; Enraf-Nonius: Delft, The Netherlands, 1990.

(71) Main, P.; Fiske, S. J.; Hull, S. E.; Lessinger, L.; Germain, G.; DeClerq, J. P.; Woolfson, M. M. *MULTAN80, A System of Computer Programs for the Automatic Solution of Crystal Structures from X-ray Diffraction Data*; University of York, England, 1980.

Table XII. Atomic Coordinates ($\times 10^4$) and Equivalent Isotropic Thermal Parameters ($\text{\AA}^2 \times 10^3$) for $[(^t\text{Bu})_2\text{Al}(\mu\text{-OH})]_3 \cdot 2\text{MeCN}$ (7)

	x	y	z	$U(\text{eq})^a$
Al(1)	-457(1)	-9390(1)	-7132(1)	22(1)
Al(2)	-3485(1)	-9163(1)	-7051(1)	23(1)
Al(3)	-1996(1)	-8272(1)	-8505(1)	21(1)
O(1)	-1964(2)	-9484(1)	-6799(1)	25(1)
O(2)	-3160(2)	-8551(1)	-7850(1)	22(1)
O(3)	-812(2)	-8810(1)	-8030(1)	23(1)
C(11)	39(3)	-10202(1)	-7646(2)	30(1)
C(12)	-506(3)	-10289(2)	-8625(2)	45(1)
C(13)	1385(3)	-10246(2)	-7643(2)	46(1)
C(14)	-359(3)	-10751(2)	-7107(3)	53(1)
C(15)	585(2)	-9004(1)	-6105(2)	28(1)
C(16)	1450(3)	-8552(2)	-6491(2)	40(1)
C(17)	1330(3)	-9478(2)	-5501(2)	44(1)
C(18)	-138(3)	-3623(2)	-5494(2)	39(1)
C(21)	-4530(3)	-9827(1)	-7659(2)	32(1)
C(22)	-5033(3)	-10270(2)	-6998(2)	49(1)
C(23)	-3884(3)	-10241(2)	-8287(2)	46(1)
C(24)	-5570(3)	-9502(2)	-8242(2)	50(1)
C(25)	-3983(2)	-8780(1)	-5935(2)	29(1)
C(26)	-3483(3)	-8117(2)	-5745(2)	38(1)
C(27)	-3577(3)	-9197(2)	-5122(2)	43(1)
C(28)	-5343(3)	-8719(2)	-5988(2)	43(1)
C(31)	-2458(3)	-8444(1)	-9813(2)	29(1)
C(32)	-3724(3)	-8217(2)	-10088(2)	55(1)
C(33)	-1667(3)	-8116(2)	-10421(2)	46(1)
C(34)	-2414(4)	-9148(2)	-10036(2)	56(2)
C(35)	-1537(2)	-7384(1)	-6179(2)	25(1)
C(36)	-2356(3)	-6906(1)	-8716(2)	38(1)
C(37)	-1570(3)	-7239(2)	-7178(2)	46(1)
C(38)	-272(3)	-7264(2)	-8390(2)	39(1)
N(1)	-5154(3)	-7747(2)	-8113(2)	56(1)
C(1)	-5974(3)	-7458(2)	-8152(2)	43(1)
C(2)	-7073(3)	-7088(2)	-8208(3)	71(2)
N(2)	1161(3)	-8698(1)	-9006(2)	52(1)
C(3)	1836(3)	-8658(2)	-9492(2)	39(1)
C(4)	2725(3)	-8586(2)	-10125(2)	52(1)

^a Equivalent isotropic U defined as $1/3$ rd the trace of the orthogonalized U_{ij} tensor.

collection was stopped after the crystals had decayed 42, 51, and 32% for a, b, and c, respectively (more respectable cut-off limits were initially used; however, the initial batch of crystal was exhausted before collection was completed). 5426 reflections were collected between the three crystals (2666, 1158, and 1602), providing 3303 unique reflections. The three data sets were scaled to provide a homogeneous set using the overlapping reflections to provide the scale factors.

Refinement based on 2358 observed reflections resulted in final values of $R = 0.0689$, $R_w = 0.0972$, and $\text{GOF} = 1.21$. One *tert*-butyl group was disordered in a 1:1 fashion, and the partial occupancy carbons were refined with isotropic thermal parameters. All other atoms were refined anisotropically. After the final cycle of least squares, the maximum shift of a parameter was less than 0.01 of its estimated standard deviation, and the final difference map showed no feature higher than $0.57 \text{ e}/\text{\AA}^3$ (close to disordered *tert*-butyl). Surprisingly, in view of the crystal decay, no solvent or region of unaccounted-for electron density was observed. The

Table XIII. Atomic Coordinates ($\times 10^4$) and Equivalent Isotropic Thermal Parameters ($\text{\AA}^2 \times 10^3$) for $[(^t\text{Bu})_2\text{Al}(\text{py})]_2(\mu\text{-O})$ (8)

	x	y	z	$U(\text{eq})^a$
Al(1)	3784(1)	8572(1)	3296(1)	22(1)
O(1)	5000	1000	5000	25(1)
C(1)	5081(3)	7962(3)	1957(3)	30(1)
C(2)	6557(3)	9547(3)	2064(3)	38(1)
C(3)	4112(4)	7043(4)	305(3)	46(2)
C(4)	5834(4)	6925(4)	2505(3)	43(1)
C(5)	1865(3)	8937(3)	2373(3)	28(1)
C(6)	2559(4)	10380(5)	1845(4)	62(2)
C(7)	1044(4)	9390(5)	3544(3)	53(2)
C(8)	498(5)	7489(5)	1077(4)	75(2)
N(1)	2685(3)	6548(2)	3829(2)	28(1)
C(9)	1690(4)	5086(3)	2776(3)	40(1)
C(10)	996(4)	3678(3)	3105(4)	51(2)
C(11)	1350(4)	3770(4)	4558(4)	51(2)
C(12)	2361(4)	5255(4)	5647(3)	47(2)
C(13)	3009(3)	5622(3)	5242(3)	34(1)

^a Equivalent isotropic U defined as $1/3$ rd the trace of the orthogonalized U_{ij} tensor.

magnitude and shape of the thermal parameters of some of the *tert*-butyl methyl groups was suggestive of rotational disorder about the C–C bond similar to that previously observed for $[(^t\text{Bu})\text{Ga}(\mu_3\text{-S})]_4$.³⁴ However, we were unable to successfully model such a disorder.

A colorless block-shaped crystal of **5** was mounted on the diffractometer, and data were collected in a method analogous to that for compounds **1**, **6**, **7**, and **8**. The unit cell was hexagonal with $a = 22.747(2)$, $c = 19.008(3)$ \AA , $V = 8518(1)$ \AA^3 , and systematic absences indicated that the space group was either $P3c1$ or $P3c1$. Attempted solution of the structure in the former showed massive disorder of the core structure. In an effort to simplify the disorder, the data were therefore solved in a lower symmetry cell solution (Pc) and partial refinement enabled location of one and a half disordered molecules, isostructural to $[\text{Na}(\text{O}^t\text{Bu})]_9$. While the structure of **5** may be sufficiently refined in the monoclinic solution to confirm the atom connectivity and is entirely consistent with all the spectroscopic characterization, the unit cell and systematic absences indicate the space group to be truly hexagonal. Since we have been unable to reconvert the monoclinic solution back up to either of the hexagonal space groups, we have not included the structural solution. We are at present attempting to obtain further crystals of **5**.

Acknowledgment. Financial support for this work is provided by the Office of Naval Research, the Aluminum Research Board (A.R.B.), and the Robert A. Welch Foundation (S.G.B.). Dr. A. P. Sattelberger (Isotope and Nuclear Chemistry Division, Los Alamos National Laboratory) and Dick Miller (Akzo Chemicals) are gratefully acknowledged for the gift of ^{17}O -enriched water and a sample of commercial MAO, respectively.

Supplementary Material Available: Full listings of bond lengths and angles, anisotropic thermal parameters, and hydrogen atom parameters (34 pages); tables of calculated and observed structure factors (110 pages). Ordering information is given on any current masthead page.